



## Ferrocenyl chalcones versus organic chalcones: A comparative study of their nematocidal activity

Saeed Attar<sup>a,\*</sup>, Zachary O'Brien<sup>a</sup>, Hasan Alhaddad<sup>b</sup>, Melissa L. Golden<sup>a</sup>, Alejandro Calderón-Urrea<sup>b</sup>

<sup>a</sup> Department of Chemistry (M/S SB-70), California State University, Fresno, CA 93740, USA

<sup>b</sup> Department of Biology (M/S SB-73), California State University, Fresno, CA 93740, USA

### ARTICLE INFO

#### Article history:

Received 7 October 2010

Revised 18 January 2011

Accepted 24 January 2011

Available online 2 February 2011

#### Keywords:

Ferrocenyl chalcone

Biological activity

Nematocidal

*Caenorhabditis elegans*

### ABSTRACT

A series of 30 organic chalcones and 33 ferrocenyl (Fc) chalcones were synthesized and characterized by melting point, elemental analysis, spectroscopy (<sup>1</sup>H NMR and FTIR) and, in two cases, by X-ray crystallography. The biological activity of each compound (10<sup>-4</sup> M in DMSO) against the model nematode *Caenorhabditis elegans* was examined in terms of % mortality (percent nematodes that died) and % fecundity (percent nematodes that reproduced) and compared to that obtained for the control medium (1% DMSO) over a 14-day period. Detailed conformational analyses for two Fc-chalcones (studied also by X-ray crystallography) were performed via molecular modeling studies. In general, the organic chalcones were found to be less polar than their Fc analogs. Some structure–activity relationships (SARs) were determined: (a) The nematocidal activities of the organic chalcones in this series were found to be much greater than those of their ferrocenyl analogs. (b) The position of the carbonyl group played a central role in the biological activity of both classes of chalcones studied. (c) For both classes of chalcones, lipophilicity of a compound seemed to play a significant role in its nematocidal activity. (d) The planarity of a ferrocenyl-chalcone seems to play a role in its activity.

Published by Elsevier Ltd.

### 1. Introduction

One of the more recent developments in organometallic chemistry has occurred at its interface with the biological sciences, hence appropriately called *bioorganometallic chemistry*.<sup>1</sup> In many of the reported examples, a phenyl group in an organic molecule with well-known biological activity has been replaced with an organometallic moiety in order to determine whether it can be made more effective. In this regard, the ferrocene derivatives have featured prominently due to their excellent stability in aqueous, aerobic media, the easy accessibility of a large variety of derivatives, and favorable electrochemical properties.<sup>2</sup> Despite some reported successes, the findings of such studies have been mixed. In some cases, the new bioorganometallic conjugate is dramatically more effective than the original organic analog, one notable example being that reported by Jaouen and co-workers on Tamoxifen (the drug used most often to treat breast cancer) and its active metabolite, hydroxytamoxifen.<sup>3a</sup> When one of the aromatic rings was replaced with a ferrocenyl group, the resulting ‘ferrocifen’ was found to be a more effective drug, possibly due to the reversible oxidation and reduction of the iron atom, which could produce hydroxyl radicals that damage DNA. On the other hand, in a sepa-

rate study,<sup>3b</sup> Jaouen et al. reported that the use of a titanocenyl-Tamoxifen conjugate led to an increased rate of growth of estrogen-dependent breast tumors because it acted like estrogen. In another set of studies, Biot and co-workers<sup>3c–e</sup> have shown that ferroquine and other ferrocenyl analogs of chloroquine (an established antimalarial compound) are very active, in vitro, against both chloroquine-sensitive and chloroquine-resistant *Plasmodium falciparum* across a variety of strains.

Chalcones are naturally occurring derivatives of the parent compound 1,3-diphenyl-2-propen-1-one (**1**, Chart 1) and belong to the flavonoid family of organic compounds.<sup>4a</sup> Chalcones have been reported to have a broad range of biological activities such as antimalarial, antibacterial, antitumor, antioxidant, antihyperglycemic, and anti-HIV.<sup>4a–1</sup> A ferrocenyl chalcone (Fc-chalcone) derivative is formed when either Ring A or B in **1** is replaced with a ferrocenyl group (e.g., **31** or **43**, Chart 2). As shown in Chart 2, two types of Fc-chalcones are generally recognized: Type 1 wherein the carbonyl group is directly attached to the ferrocenyl ring, and Type 2 wherein the carbonyl group is attached to the phenyl ring. For the purpose of comparing the structure–activity relationships (SARs) of the organic chalcones with those of the ferrocenyl analogs, the compounds in the organic series have also been divided into two types (Chart 1), depending on whether the phenyl ring attached to the carbonyl carbon is substituted (Type 2) or not (Type 1).

\* Corresponding author. Tel.: +1 559 278 2639; fax: +1 559 278 4402.

E-mail address: [sattar@csufresno.edu](mailto:sattar@csufresno.edu) (S. Attar).

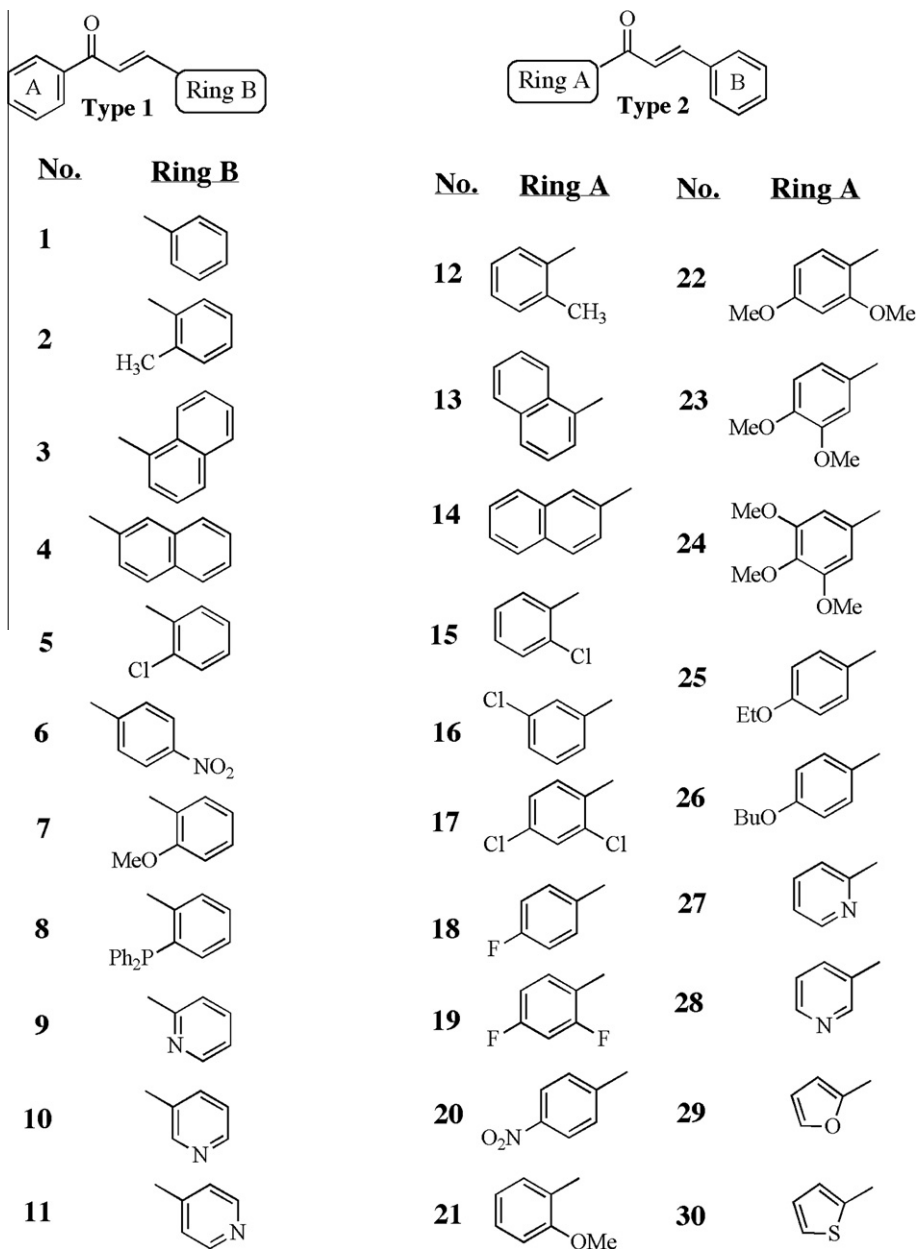


**Chart 1.** Structures of the organic chalcones (1–30) prepared for this study.

Despite the fact that Fc-chalcones have been known since the 1960s,<sup>5</sup> only two studies on their biological activity have been conducted so far.<sup>6</sup> In a preliminary paper,<sup>6a</sup> followed by a full account,<sup>6b</sup> Go and co-workers have reported on the synthesis of a series of Fc-chalcones and the evaluation of their in vitro antimalarial (antiplasmodial) activity against a chloroquine-resistant strain of *P. falciparum*. These authors found that, in general, Type 1 Fc-chalcones were more active than their Type 2 isomers; for example, **37** (Ring B = 4-nitrophenyl;  $IC_{50}$  = 5.1  $\mu$ M) was found to be much more active than **52** (Ring A = 4-nitrophenyl;  $IC_{50}$  = 61.7  $\mu$ M). However, if a heterocyclic ring was part of the molecule, then the Type 2 compound was more active than its Type 1 isomer; for example, **60** (Ring A = 3-pyridinyl;  $IC_{50}$  = 4.5  $\mu$ M) was more active than its Type 1 isomer, **18** (Ring B = 3-pyridinyl;  $IC_{50}$  = 17.0  $\mu$ M) and the most active among all Fc-chalcones studied. In addition, it was found that **31** (Ring B = Ph;  $IC_{50}$  = 19  $\mu$ M) was much more active than **43** (Ring A = Ph,  $IC_{50}$  = 175  $\mu$ M). However, in terms of the antimalarial activity, the Fc-chalcones

investigated were found to be less active than their organic analogs as previously reported by Go and co-workers as well.<sup>4a</sup> Finally, Sohar and co-workers<sup>6c</sup> have reported on the synthesis of some glycoside derivatives of Fc-chalcones and Fc-pyrazolines and their in vitro antitumor activity against human leukemia (HL-60) cells. It was found that four of the chalcone derivatives containing either a ferrocenyl moiety and a *p*-hydroxyphenolic ring or a size-independent apolar substitution of the ferrocene ring showed promising antitumor properties.

Nematodes are ubiquitous throughout the world, populating moist environments that include plant and animal tissues. Plant pathogenic nematodes account for a loss of about \$80 billion to agriculture every year.<sup>7</sup> The most common solution for the control of plant pathogenic nematodes, as well as other soil pests, has been the use of the common fumigant, methyl bromide ( $CH_3Br$ ).<sup>8a,b</sup> However, this compound accumulates in the upper atmosphere and can contribute to stratospheric ozone depletion when photolyzed into free radicals by high-energy ultraviolet radiation.<sup>8a</sup> For

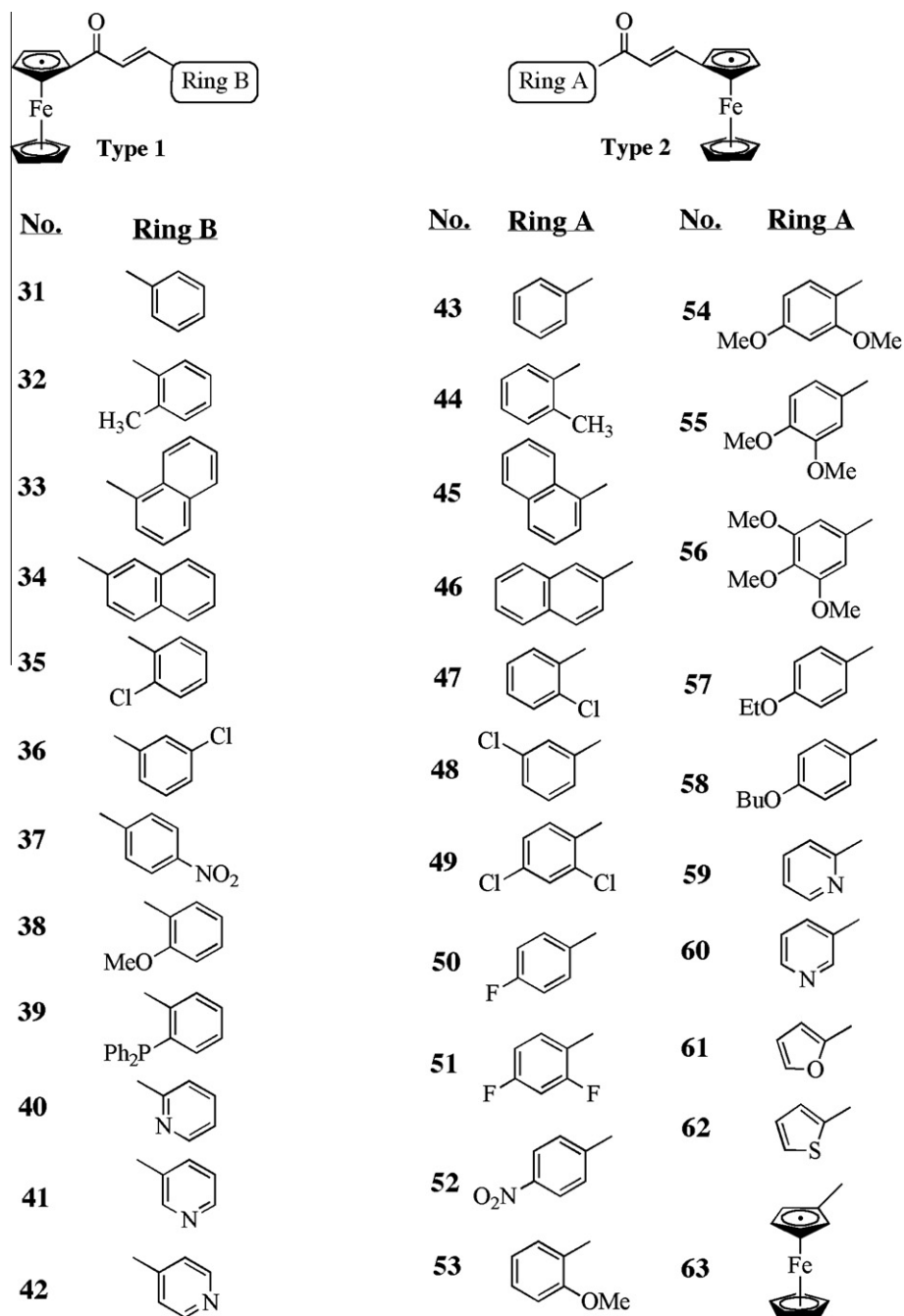


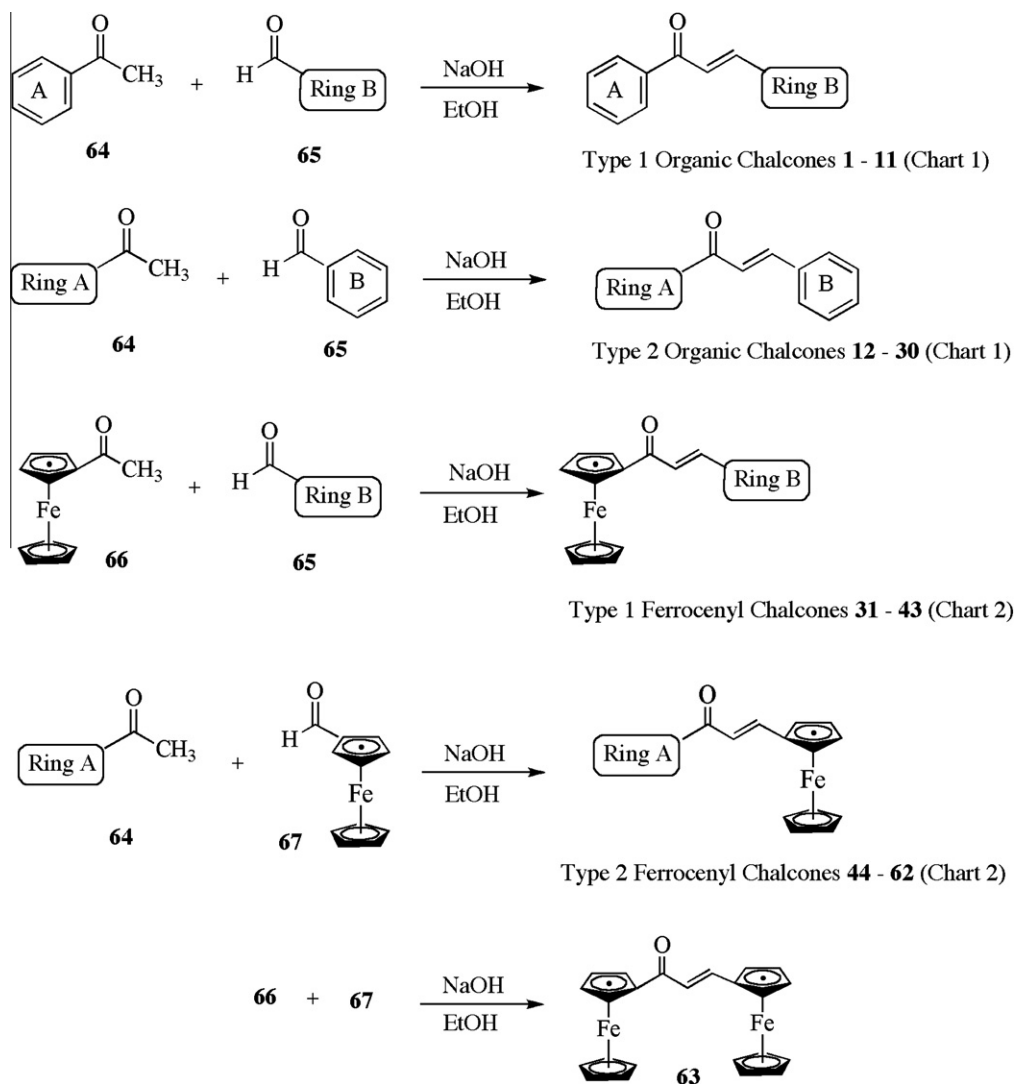
Chart 2. Structures of the ferrocenyl chalcones prepared for this study.

that reason, as of 2005, the use of methyl bromide has been phased out as an agricultural fumigant in developed countries according to the guidelines of the Montreal Protocol.<sup>8b-d</sup> However, despite the current ban on the use of methyl bromide, it is still widely used throughout the agriculture industry by way of exemptions since no effective alternative has been found as yet.<sup>8d</sup>

There have been a few published reports on the nematocidal activity of organic chalcones. As early as 1967, Laliberté et al.<sup>9a</sup> reported that (*E*)-chalcone (**1**, Chart 1) and other related compounds showed high activity against zooparasitic nematodes *Syphacia obvelata* and *Notodiptomus dubius* (pinworms in mice). Gonzalez et al.<sup>9b</sup> reported that **1**, and other similar aromatic compounds related to the Shikimate pathway, showed activity against phytoparasitic species *Globodera pallida* and *Globodera rostochiensis* (potato-cyst nematodes) and that the observed biological activity was due

to the presence of a conjugated carbonyl system in each of these molecules. In a later report,<sup>9c</sup> the same authors found that not only was compound **1** highly toxic for the two nematodes mentioned ( $CL_{50} = 33$  mM), but that it also acted as a potent inhibitor of nematode hatch ( $HIC_{50} = 7$  mM).

Considering the reported nematocidal properties of organic chalcones,<sup>9</sup> and the general dearth of information on the biological activity of Fc-chalcones,<sup>6</sup> we became interested in conducting a study on their nematocidal activities as compared to those of their organic analogs. As shown in Charts 1 and 2, a total of 63 chalcones were synthesized and their biological activities against *Caenorhabditis elegans* nematodes were determined. The free-living *C. elegans* was chosen as a model for studying the nematocidal activities of compounds **1–63** primarily due to the ease with which it can be handled. This soil nematode, which is about 1 mm long, is found



**Scheme 1.** Synthesis of organic and Fc-chalcones.

in temperate regions of the planet.<sup>10a</sup> It was first used in the 1960s for studies on the genetics of development and neurobiology and since then it has been used increasingly as a model system for parasitic nematodes and higher organisms where defining the function of genes of interest can be difficult due to lack of appropriate knock-out approaches or suitable functional assays.<sup>10b</sup> These nematodes pose no threat to the researcher, can thrive at room temperature, reproduce quickly, and have short life spans (~15 days). In addition, as Holden-Dye and Walker<sup>10c</sup> have pointed out, *C. elegans* is no more dissimilar to parasitic nematodes than each individual species of parasite is to another. Thus, all of the mentioned factors made *C. elegans* an ideal organism for our study. Herein, we wish to report on the results of our combined chemical and biological investigations on the two sets of chalcone derivatives shown in [Charts 1 and 2](#).

## 2. Results and discussion

### 2.1. Chemistry

#### 2.1.1. Synthesis

As shown in [Scheme 1](#), chalcones can be readily synthesized via the classical base-catalyzed Claisen–Schmidt condensation reaction<sup>4a</sup> in ethanol solvent. Thus, starting from the appropriate

acetophenone derivative (**64** or **66**) and benzaldehyde derivative (**65** or **67**), chalcones **1–62** have been prepared, with percent yields generally in the 70–80% range after chromatography and/or crystallization. In addition, 1,3-diferrocenyl-2-propen-1-one (**63**), wherein both rings A and B are ferrocenyl groups, was also synthesized from the combination of **66** and **67** in order to make a direct comparison to its diphenyl analog (**1**). The purity of each compound was confirmed by <sup>1</sup>H NMR spectroscopy, melting point determination, and TLC analysis, in addition to elemental analysis for thirteen new Fc-chalcones prepared for this study, as described in [Section 4](#).

#### 2.1.2. Structural characterization by spectroscopy

Some of the structural features of chalcones, as determined via their spectral properties, may aid us in explaining certain aspects of their observed biological activity. The <sup>1</sup>H NMR and IR spectral data for the organic and Fc-chalcones are presented in [Table 1A and B](#), respectively, and their salient features are discussed below.

The synthesis of chalcones via the Claisen–Schmidt condensation leads to the exclusive formation of the (*E*)-stereoisomer, which is a result of the more favorable *anti* periplanar elimination of the hydroxide group from the carbanion intermediate in this reaction. The predominance of the (*E*) configuration at the C=C bond of chalcones has been established via <sup>1</sup>H NMR spectroscopy.<sup>4a,11a</sup> The

**Table 1A**  
Spectral data for organic chalcones **1–30**

Compd	NMR			FT-IR	
	$\delta_{H\alpha}$	$\delta_{H\beta}$	$^3J_{H\alpha H\beta}$ (Hz)	$\nu_{C=O}$ (cm <sup>-1</sup> )	$\nu_{C=C}$ (cm <sup>-1</sup> )
<b>1</b>	7.52	7.80	15.8	1661	1607
<b>2</b>	<sup>a</sup>	8.04	15.4	1662	1597
<b>3</b>	<sup>a</sup>	8.20	15.4	1652	1589
<b>4</b>	7.34	7.76	15.6	1660	1592
<b>5</b>	<sup>a</sup>	7.80	15.8	1668	1605
<b>6</b>	7.66	7.82	16.0	1667	1610
<b>7</b>	7.37	8.14	15.9	1658	1592
<b>8</b>	<sup>a</sup>	7.99	16.0	1682	1578
<b>9</b>	7.77	8.12	15.4	1669	1610
<b>10</b>	7.62	7.80	15.8	1667	1603
<b>11</b>	7.54	8.03	15.7	1683	1602
<b>12</b>	7.35	7.89	15.4	1667	1575
<b>13</b>	7.47	7.85	15.4	1657	1592
<b>14</b>	7.29	7.83	15.4	1654	1586
<b>15</b>	7.33	7.91	15.7	1646	1596
<b>16</b>	7.47	8.02	15.8	1662	1602
<b>17</b>	7.43	7.61	15.8	1680	1592
<b>18</b>	7.26	7.81	16.0	1663	1605
<b>19</b>	7.65	7.91	16.0	1651	1603
<b>20</b>	7.47	7.81	15.7	1661	1585
<b>21</b>	7.36	7.84	15.9	1659	1600
<b>22</b>	7.34	7.84	16.0	1654	1585
<b>23</b>	7.27	7.87	15.4	1655	1594
<b>24</b>	7.27	7.90	15.4	1678	1583
<b>25</b>	7.48	7.88	15.6	1672	1607
<b>26</b>	7.56	8.04	15.7	1669	1605
<b>27</b>	7.95	8.33	16.2	1668	1607
<b>28</b>	7.52	7.86	15.8	1683	1652
<b>29</b>	7.4	7.40	15.6	1652	1590
<b>30</b>	7.26	7.26	15.6	1650	1583

<sup>a</sup> The NMR signal for this proton was obscured by the overlapping signals in the aromatic region.

magnitude of the coupling constant ( $^3J_{HH} \sim 15\text{--}16\text{ Hz}$ )<sup>11a</sup> for the two vinylic protons (those attached to C $\alpha$  and C $\beta$ ; Scheme 2A) has been used to verify the (*E*)-configuration. As seen in Table 1A and B, all chalcones prepared in this study exhibit the expected (*E*)-stereochemistry at their C=C bonds, with the magnitude of the coupling constant ( $^3J_{H\alpha H\beta}$ ) being in the expected range. It is noted that the chemical shift of H $\beta$  is greater than that of H $\alpha$  throughout both series of chalcones. This is explained by the existence of a formal positive charge on C $\beta$  (Scheme 2A), formed as a result of resonance distribution of *p*-electron density in going from one canonical form (**1a**) to another (**1b**), which causes the shift of H $\beta$  signal to lower fields. There is no other discernable trend in the magnitude of either  $\delta_{H\alpha}$  or  $\delta_{H\beta}$  as a function of the nature of the substituent on either phenyl ring in Type 1 and Type 2 chalcones of both series. It should also be noted that the configuration at the C=C bond of a chalcone can play a significant role in its biological activity.<sup>11a</sup> For example, Larsen et al.<sup>11b</sup> have prepared a series of chalcones analogues, locked in either the (*Z*) or the (*E*) form, and evaluated their antiplasmodial activity. It was shown that the (*Z*)-locked analogues were nearly inactive, whereas the (*E*)-locked analogues were equipotent to the parent chalcones, indicating that the (*E*)-form is the active stereoisomer.

In addition to the configuration at the C=C bond of the enone systems represented by chalcones, there exist two limiting conformers, *s-cis* and *s-trans* that result from free rotation about the C1–C2 bond in such molecules (Scheme 2B).<sup>4a,11b</sup> This has been confirmed through X-ray crystallography,<sup>4a</sup> IR spectroscopy,<sup>11g</sup> and computational methods.<sup>11g</sup>

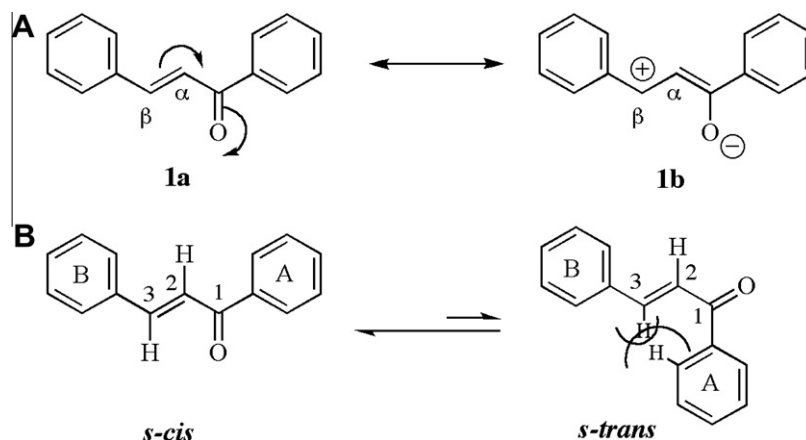
An un-substituted enone exists predominantly in the *s-cis* conformation (both in solution and in the solid state) because the *s-trans* conformer is disfavored thermodynamically due to the steric interaction between the H atom attached to C3 and that on the

**Table 1B**  
Spectral data for Fc-chalcones **31–63**

Compd	NMR			FT-IR	
	$\delta_{H\alpha}$	$\delta_{H\beta}$	$^3J_{H\alpha H\beta}$ (Hz)	$\nu_{C=O}$ (cm <sup>-1</sup> )	$\nu_{C=C}$ (cm <sup>-1</sup> )
<b>31</b>	7.14	7.81	15.8	1652	1595
<b>32</b>	7.14	7.78	15.6	1652	1592
<b>33</b>	7.24	8.69	15.3	1650	1596
<b>34</b>	7.25	7.98	15.3	1650	1586
<b>35</b>	7.07	8.10	15.8	1643	1604
<b>36</b>	6.74	7.71	15.1	1661	1603
<b>37</b>	7.20	7.82	15.4	1654	1605
<b>38</b>	7.07	8.10	15.5	1656	1581
<b>39</b>	7.02	7.68	15.1	1650	1588
<b>40</b>	7.46	7.72	15.4	1654	1605
<b>41</b>	7.18	7.78	15.6	1656	1607
<b>42</b>	7.20	7.77	15.6	1662	1608
<b>43</b>	7.13	7.76	15.1	1655	1586
<b>44</b>	7.04	7.50	15.6	1657	1589
<b>45</b>	6.89	7.47	15.8	1658	1591
<b>46</b>	7.29	7.83	15.6	1652	1584
<b>47</b>	6.70	7.33	15.4	1639	1591
<b>48</b>	7.06	7.81	15.2	1656	1582
<b>49</b>	6.67	7.34	15.8	1644	1584
<b>50</b>	7.11	7.78	15.1	1655	1600
<b>51</b>	7.21	7.84	15.9	1655	1595
<b>52</b>	7.08	7.83	15.4	1650	1573
<b>53</b>	7.08	7.74	15.8	1650	1600
<b>54</b>	7.06	7.56	15.8	1649	1603
<b>55</b>	7.15	7.74	15.4	1652	1575
<b>56</b>	7.07	7.75	15.1	1649	1570
<b>57</b>	7.15	7.75	15.2	1651	1588
<b>58</b>	6.61	7.63	15.2	1675	1602
<b>59</b>	7.74	8.19	15.8	1661	1592
<b>60</b>	7.08	7.83	15.8	1656	1589
<b>61</b>	7.02	7.79	15.6	1644	1582
<b>62</b>	7.03	7.80	15.4	1642	1575
<b>63</b>	6.75	7.71	15.5	1646	1577

ortho position of the phenyl group (Scheme 2B).<sup>4a,11</sup> However, the position of the equilibrium shown in Scheme 2B can be shifted by the appropriate substitution of the enone system. Thus, an alkyl substituent at C2 favors the *s-trans* conformer, while the existence of such a substituent at C3 favors the *s-cis* conformer. In addition, an increase in the steric bulk of the phenyl group attached to the carbonyl carbon favors the *s-cis* conformer regardless of other substituents at C2 or C3. Furthermore, increasing the solvent's polarity is generally expected to favor (stabilize) the *s-trans* conformer since it is more polar than its *s-cis* counterpart.

The IR data (Tables 1A and 1B) show that while the electron-withdrawing or -donating properties of the two rings in a chalcone may vary, the magnitudes of the stretching frequencies of the C=O or C=C bonds are remarkably comparable. For example, among Type 1 organic chalcones (**1–11**), wherein the nature of the substituent on the 'A' ring changes from the weakly electron-donating CH<sub>3</sub> group in **2** to the highly electron-withdrawing NO<sub>2</sub> group in **6**, the magnitude (cm<sup>-1</sup>) of  $\nu_{C=O}$  varies as follows: **2** (1662), **3** (1652), **4** (1660), **5** (1668), and **6** (1667). In addition, the location of the carbonyl group in the chalcone molecule does not seem to greatly affect the position of the stretching frequency band assigned to this group. For example, the magnitude of  $\nu_{C=O}$  among the eight pairs of isomeric organic chalcones listed in Chart 1 varies as follows: **2** (1662) and **12** (1667), **3** (1652) and **13** (1657), **4** (1660) and **14** (1654), **5** (1668) and **15** (1646), **6** (1667) and **20** (1661), **7** (1658) and **21** (1659), **9** (1669) and **27** (1668), **10** (1667) and **28** (1683). The  $\nu_{C=C}$  values also show little variation among the organic chalcones. Similar observations are made regarding the magnitudes of both  $\nu_{C=O}$  and  $\nu_{C=C}$  among the Fc-chalcones **31–63**. The general conclusion one can draw from the aforementioned discussion on the NMR and IR properties of these chalcones is that the basic structure of these



Scheme 2. For (*E*)-chalcone (**1**): (A) two canonical forms; (B) two limiting conformations.

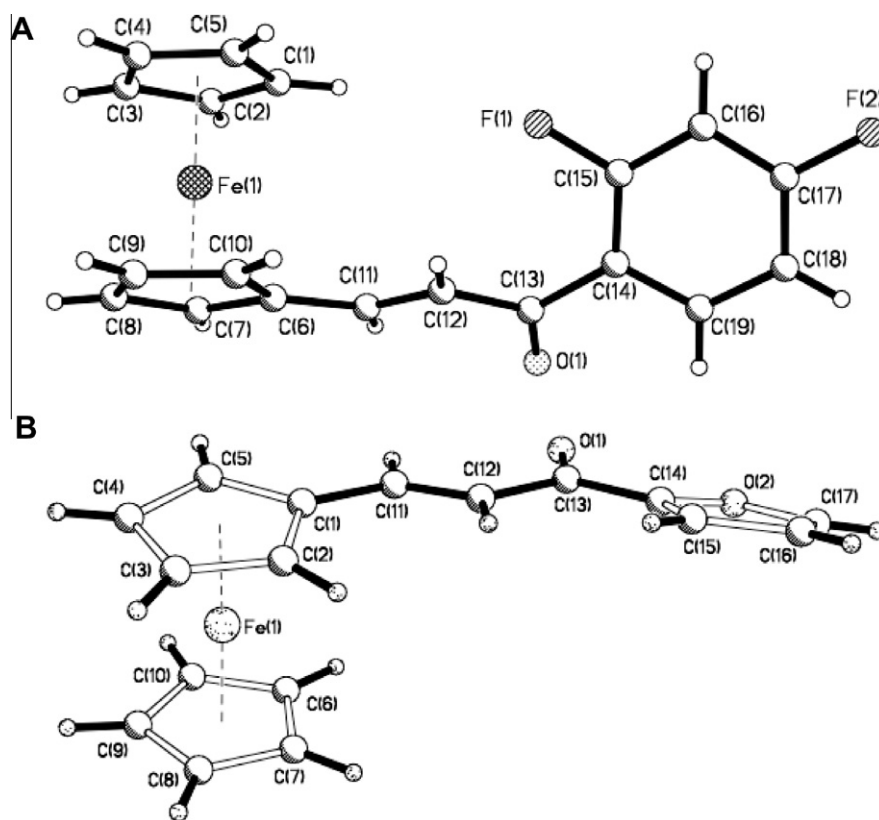


Figure 1. (A) Molecular structures of 1-(2,4-difluorophenyl)-3-ferrocenyl-2-propen-1-one (**51**); (B) molecular structure of 1-(2-furanyl)-3-ferrocenyl-2-propen-1-one (**61**).

chalcones is remarkably similar despite changes in the steric and electronic nature of the phenyl rings.

Finally, it should be noted that despite attempts to precisely determine the *s-cis/s-trans* equilibrium ratio using IR spectroscopic data, obtaining reliable information and drawing definitive conclusions from such data has proven difficult.<sup>11d</sup> What is clear from all published studies on this structural aspect of chalcones is that while the *s-cis* conformer predominates in solution for most chalcones studies to date, the equilibrium concentration of the *s-trans* conformer is substantial. A discussion of the *s-cis/s-trans* ratio of a chalcone in solution becomes relevant in light of recent studies that have revealed the significant role that such conformational changes can play in a chalcone's biological activity.<sup>12a,c,41</sup>

### 2.1.3. Structural characterization by X-ray crystallography

The solid-state structures of two Fc-chalcones prepared in our work (**51** and **61**) have unequivocally been determined by X-ray crystallography. The structures are shown in Figure 1A and B, respectively, and their selected structural parameters are presented in Table 2.

As shown in Table 2, all the bond lengths and angles are within the normal range found for such molecules in previous studies.<sup>4a</sup> For example, the C=O bond length is 1.244 Å in **51** and 1.266 Å in **61**. The bond angle around the carbonyl carbon, that is, C(12)–C(13)–C(14), is 119.49° in **51** and 115.3° for **61**, both very close to the ideal value of 120°. Each structure in Figure 1 shows the expected (*E*)-stereochemistry of the C=C bond and the *s-cis* conformation of the enone portion of each molecule. The extent of

**Table 2**  
Selected structural parameters for Fc-chalcones **51** and **61**

Compound	<b>51</b>	<b>61</b>
<i>Bond lengths (Å)</i>		
C(11)–C(12)	1.334(3)	1.316(16)
C(12)–C(13)	1.463(2)	1.477(15)
C(13)–O(1)	1.244(2)	1.266(12)
C(13)–C(14)	1.494(3)	1.491(16)
<i>Bond angles (°)</i>		
C(12)–C(11)–C(6)	125.36(17)	
C(12)–C(11)–C(1)		127.9(9)
C(11)–C(12)–C(13)	120.73(17)	124.3(10)
O(1)–C(13)–C(12)	121.97(17)	122.7(10)
O(1)–C(13)–C(14)	118.52(16)	122.0(10)
C(12)–C(13)–C(14)	119.49(16)	115.3(9)
<i>Torsion angles</i>		
C(10)–C(6)–C(11)–C(12)	–4.4	
C(2)–C(1)–C(11)–C(12)		–11.2
C(6)–C(11)–C(12)–C(13)	174.60	
C(1)–C(11)–C(12)–C(13)		178.7
C(11)–C(12)–C(13)–O(1)	–21.7	–0.6
C(11)–C(12)–C(13)–C(14)	159.3	–179.0
C(12)–C(13)–C(14)–C(15)	–32.6	–16.3
C(12)–C(13)–C(14)–C(19)	150.6	
C(12)–C(13)–C(14)–O(2)		166.3

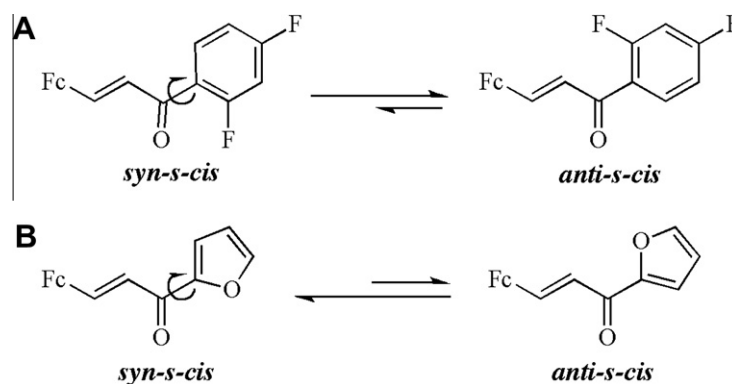
planarity of the enone portion of each molecule is different. As shown in Table 2, the magnitude of the derived torsion angle C11–C12–C13–O(1) in **51** ( $-21.7^\circ$ ) is substantially different from that in **61** ( $-0.6^\circ$ ). This indicates that the carbonyl group is significantly twisted out of the plane of the adjacent 2,4-difluorophenyl ring in **51**, but that it is essentially in the same plane as that of the furanyl ring in **61**. In fact, the difference between these two particular torsion angles is the largest among those listed in Table 2. The larger magnitude of the carbonyl stretching frequency of **51** ( $1655\text{ cm}^{-1}$ ), as compared to that of **61** ( $1644\text{ cm}^{-1}$ ; Table 1B), is indicative of the greater deviation from planarity of the enone portion of **51** relative to that of **61**. This is due to the fact that the greater planarity of the enone portion allows for more extended

delocalization of the pi electrons of the C=O and C=C bonds (Scheme 2A) which, in turn, reduces the double-bond character of the carbon–oxygen bond leading to a lower magnitude of  $\nu_{\text{C=O}}$  for **61**. The reduction in the pi-electron density of the C=O bond in going from **51** to **61** is accompanied by a concomitant increase in the length of this bond, (**51**, 1.244 Å; **61**, 1.266 Å). The greater planarity of **61** may play a significant role in its higher nematocidal activity as compared to that of **51** (vide infra). A search of the contents of *Chemical Abstracts* via the *SciFinder Scholar*™ service<sup>13</sup> revealed that seven other crystal structures of Fc-chalcones have been reported so far. These include structures of compounds **34**,<sup>14a</sup> **37**,<sup>6b</sup> **43**,<sup>6b</sup> **58**,<sup>6b</sup> two anthracenyl derivatives,<sup>14b</sup> and a dipyrrenyl derivative.<sup>14c</sup> It is also noteworthy that the structure of **61** (Fig. 1B) represents the first such determination for a heterocyclic derivative of an Fc-chalcone. The structures shown in Figure 1A and B confirm the (*E*)-stereochemistry at the C=C bond, as well as the *s-cis* conformation of the enone portion, in each of these molecules. In addition, the structure of **51** shows that it has adopted the *anti* conformation with respect to the position of the *ortho*-F atom on the phenyl ring relative to that of the C=O group, hence the *anti-s-cis* designation (Scheme 3A). This can be explained in terms of the steric repulsion between these two groups in the *syn* conformer versus that in the *anti* conformer. As for compound **61**, the preferred solid-state conformation is one in which the oxygen atom of the furanyl ring is in a *syn* position relative to that of the C=O group, hence the *syn-s-cis* designation (Scheme 3B). A similar observation has been made in a thiophenyl derivative of chalcone and has been explained in terms of an attractive electrostatic interaction between the sulfur atom of the thiophene ring and the oxygen atom of the carbonyl group.<sup>15</sup> More will be discussed about this structural aspect of **51** and **61** in Section 2.3.

## 2.2. Biology

### 2.2.1. Experimental setup

Prior to starting the studies on the biological activity of the chalcones **1–63**, the testing solution had to be optimized. As ex-



**Scheme 3.** (A) Conformations of the substituted phenyl ring in **51**; (B) conformations of the furanyl ring in **61**.

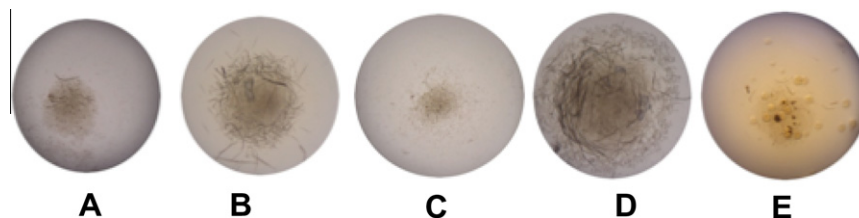


**Figure 2.** Appearance of *C. elegans* nematodes at different stages of the 14-day test under a dissecting microscope: (A) alive nematodes; (B) alive and reproduced nematodes; (C) dead nematodes; (D) dead and reproduced nematodes; (E) yeast-contaminated well.

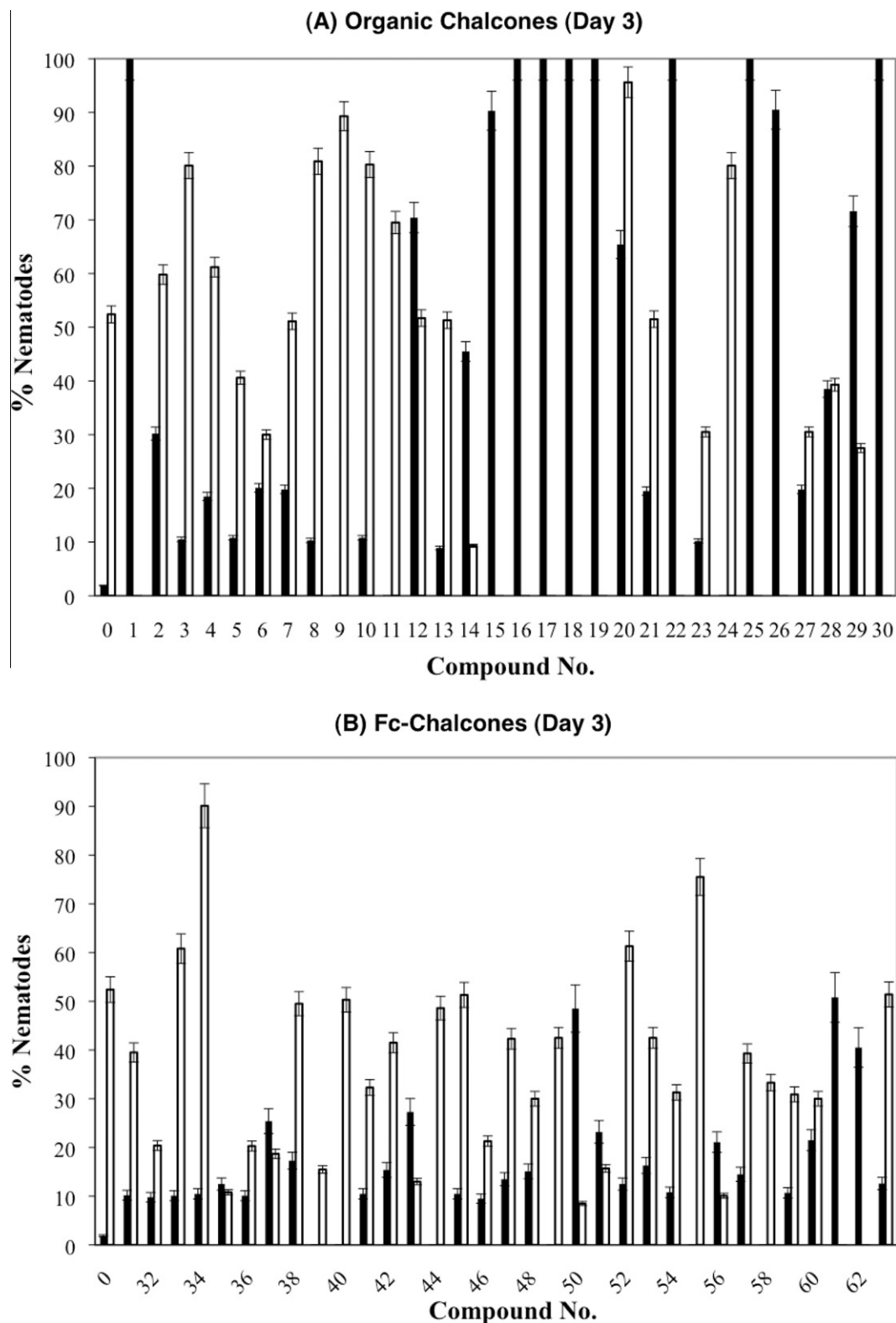


**Figure 3.** Comparison between the effect of (A) organic- and (B) Fc-chalcones on nematodes on day 3 of their exposure. Black bars: % mortality (% nematodes dead); white bars: % fecundity (% nematodes reproduced); compound zero is the DMSO control; absence of any bar for a given compound indicates no detectable activity.

pected, the Fc-chalcones (31–63) were found to be water-insoluble due to the presence of a hydrophobic fragment in each. Dimethyl sulfoxide (DMSO) was therefore chosen since, as a polar aprotic solvent, it dissolves most organic compounds and is miscible with water. Before any testing of the Fc-chalcones could commence, a

negative control solution had to be prepared. This required the determination of a minimum concentration of DMSO in the liquid medium that did not cause death or inhibit the reproduction of the *C. elegans* nematodes in our study. Thus, ten repetitions of each of the four different DMSO solutions (50%, 10%, 2%, and 1% by

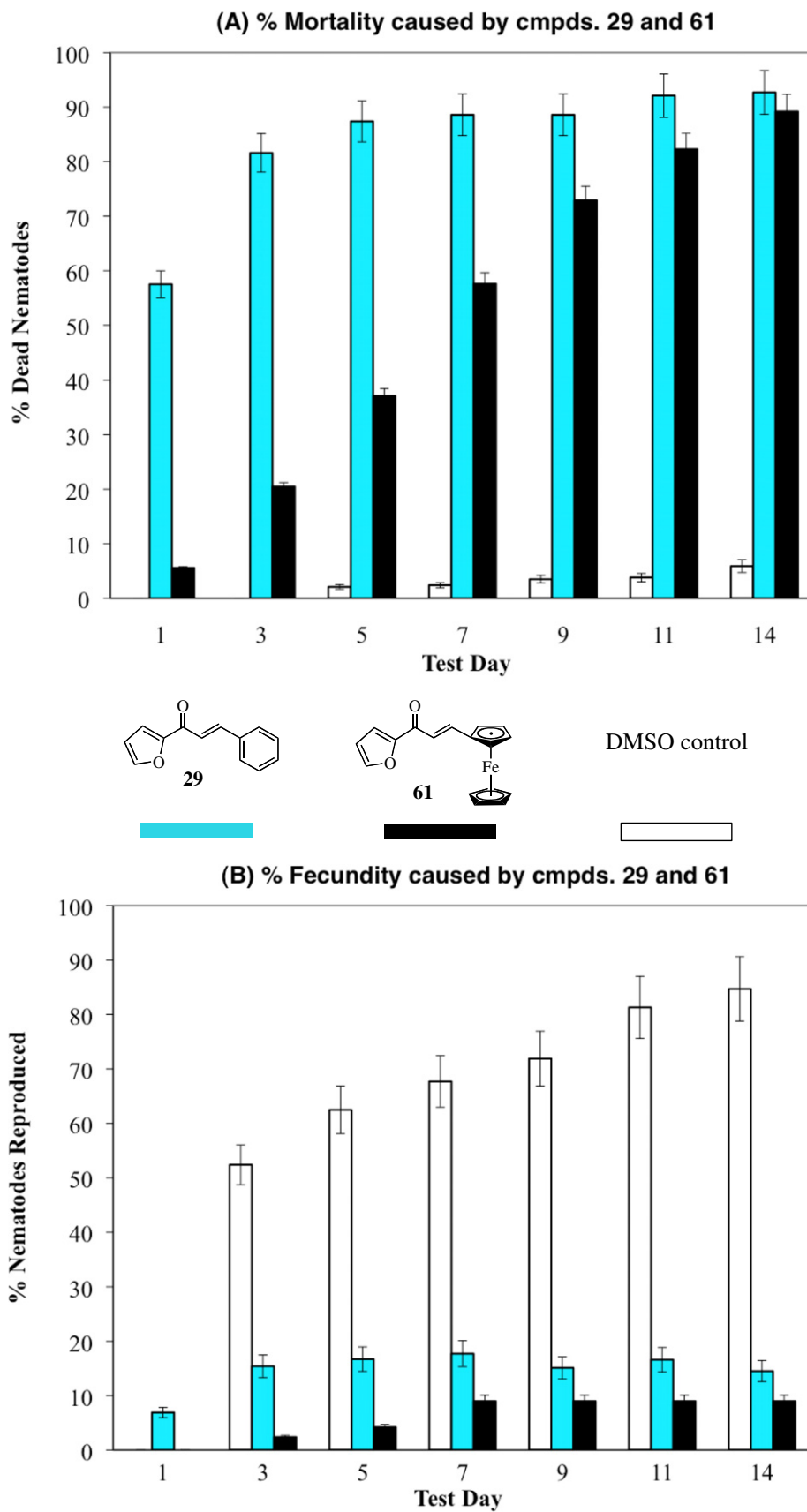


**Figure 4.** Comparison between the biological activity against *C. elegans* nematodes of an organic chalcone (**29**) and a ferrocenyl chalcone (**61**), both relative to that of a control solution (DMSO); (A) % mortality, (B) % fecundity; average values from triplicate sets of 96-well microtiter plates over 14 days; absence of any bar indicates no activity.

volume), placed in liquid nematode medium, were tested. It was found that 1% was the maximum concentration of DMSO in liquid nematode medium that did not have any adverse biological effects on the nematodes. Each test was run for 14 days since the nematodes were placed into the testing solution 1 day after synchronization and their average life span is 15 days. Results obtained from leaving the nematodes in the testing solution any longer than two weeks would not be particularly meaningful because most of them would be dead by then regardless of the presence of a nematocidal agent.<sup>16</sup>

In order to determine the minimum inhibitory concentration (MIC) of the Fc-chalcones **31–63**, they were initially tested at  $10^{-6}$  and  $10^{-5}$  M concentrations but no effect was observed in each case. However, when the concentration was increased to  $10^{-4}$  M, biological activity was observed. A concentration of  $10^{-3}$  M was also attempted but the results were very similar to the those obtained at  $10^{-4}$  M, in addition to the fact that the  $10^{-3}$  M solution had a layer of crystals (presumably of Fc-chalcones) on the bottom of the vessel. This suggested to us that a  $10^{-4}$  M concentration is near the saturation point of Fc-chalcones in DMSO. Subsequent to the determination of MIC for Fc-chalcones, all compounds (**1–63**) were tested at a concentration of  $10^{-4}$  M in order to make a valid comparison between the nematocidal activity of ferrocenyl chalcones and their organic analogs.

A bioassay was constructed to test the ability of the compounds to kill the worms (% mortality) and to inhibit their reproduction (% fecundity). Each compound was screened for effectiveness by first testing it on 10 nematodes at a time in parallel with a set of ten worms in a control solution (1% DMSO + 99% liquid worm medium without any test compound). Each test well (experiment or control) was monitored over a 14-day period (days 1, 3, 5, 7, 9, 11, and 14 after incubation). Figure 2 shows the typical appearance, under a dissecting microscope, of *C. elegans* nematodes at different stages of the 14-day test.

During a given test, the viability of each nematode was assessed under a dissecting microscope by disturbing it with a probe and looking for movement; percent mortality was then calculated for each chalcone. In the same fashion, percent fecundity for each chalcone was determined by counting the number of reproduced nematodes.

### 2.2.2. Results of the biological studies

The results (% mortality and % fecundity) of the preliminary screening of compounds **1–63**, obtained on the third day of incubation, are presented in Figure 3A and B.

Day 3 was chosen for this purpose because that seemed to be the appropriate time after incubation when the biological effects of a given compound on *C. elegans* nematodes could easily be observed. In these tests, we looked for compounds with significant biological activity, that is, those compounds that caused high % mortality (nematode death) and low % fecundity (nematode reproduction) relative to the control (DMSO) solution.

At the first glance of Figure 3, it becomes immediately obvious that the organic chalcones are, as a class, more active than their ferrocenyl analogs. For example, whereas eight organic chalcones (**1**, **16**, **17**, **18**, **19**, **22**, **25**, and **30**) showed 100% mortality (hence 0% fecundity) on the third day, none of the Fc-chalcones showed that type of activity relative to the results obtained for the control solution (compound '0' in Fig. 3A and B; 1.9% mortality, 52.5% fecundity). Other organic chalcones with significant nematocidal activity were **15**, **26**, and **29**. Among Fc-chalcones, compounds **37**, **43**, **50**, **51**, **56**, **61**, and **62** showed significant biological activity, with **61** showing the highest activity (52.3% mortality, 0.0% fecundity). Another trend that is revealed in both Figure 4A and B is that, for both classes of chalcones, Type 2 compounds appear to be more active than Type 1 analogs. This points towards certain

structure–activity relationships (SARs), as discussed later in this report.

Since investigating the nematocidal activity of Fc-chalcones was the focus of this study, we decided to take a closer look at those compounds that had shown significant activity in the preliminary screening (i.e., **37**, **43**, **50**, **51**, **56**, **61**, and **62**). Thus, in order to obtain statistically relevant data, each of these seven compounds was tested (in triplicate) using 96 nematodes, that is, one nematode in each well of a 96-well microtiter plate, in parallel to a set of 96 controls as described before. Although compounds **37**, **43**, **51**, and **56** had exhibited promising biological activity in the preliminary tests (Fig. 3B), each yielded results very similar to the DMSO control in the larger-scale tests, that is, many nematodes reproduced quickly and almost all survived. Thus, only Fc-chalcones **50**, **61**, and **62** were found to show significant activity relative to the DMSO control. For comparison, the activities of the organic analogs of these three compounds, that is, **18**, **29**, and **30** were also determined. Plots of % mortality (A) or % fecundity (B) versus test day (1–14) for compounds **29** and **61**, shown in Figure 4A and B, are representative of all three pairs of compounds.

Comparing the activities of the three pairs of compounds specified above, as represented by Figure 4A and B, reveals a few trends. First, with respect to % mortality of nematodes, the organic chalcones were found to be more active than their ferrocenyl analogs and seemed to exert their nematocidal influence at a much faster rate (100% mortality for **18** and **30** on the first day of incubation versus 92.0% for **62** on the 14th day).

Second, with respect to % fecundity (Figs. 5B, 6B and 7B), the six chalcones studied resulted in significantly lower numbers of reproduced nematodes compared to the control and this activity, when exhibited, remained fairly constant throughout the 14-day testing period.

### 2.3. Molecular modeling studies

Molecular modeling studies can provide useful information that could be used in elucidating the structure–activity relationships (SARs). There have been many reports involving molecular modeling studies of organic chalcones,<sup>12c,17</sup> but only one on their ferrocenyl analogs.<sup>6b</sup> We chose compounds **51** and **61** for this purpose for two reasons. First, we were able to use the structural parameters (especially the torsion angles) obtained through X-ray crystallography as starting points to build their molecular models. Second, although both **51** and **61** are Type 2 Fc-chalcones, they exhibited significantly different biological activities in the preliminary screening as shown in Figure 3B (**51**: 23.2% mortality, 15.7% fecundity; **61**: 50.8% mortality, 0% fecundity). Therefore, a conformational analysis of these two compounds could reveal structural features that play a role leading to such varied activity. Thus, molecular models were built and optimized via the semi-empirical PM-3 method (using software *Spatan '08*<sup>TM</sup>).<sup>18</sup> The conformational profile of each compound was then determined by varying each of the three torsion angles ( $\theta_1$ ,  $\theta_2$ ,  $\theta_3$ ; Table 3) in steps of  $15^\circ$ , with energy minimization in each step, while constraining the other two angles. The results of these studies on the conformational energy changes, along with the corresponding variation in the magnitude of dipole moment ( $\mu$ ) for each conformer, are numerically shown in Table 3 and graphically presented in Figures 5 and 6.

#### 2.3.1. Conformational analysis of compound 51

Rotation around the C13–C14 bond in **51** generates the torsion angle  $\theta_1$  (defined by C12–C13–C14–C15 atoms). As seen in Figure 5A (solid line with circles), this rotation produces two minima, one at  $\theta_1 = 240^\circ$  ( $-120^\circ$ ) and the other at  $\theta_1 = 315^\circ$  ( $-45^\circ$ ). (Note: The positive and negative signs denote the clockwise and counter-clockwise rotations of the torsion angle, respectively, and can be

**Table 3**  
Results of the conformational analysis<sup>a-d</sup> studies for **51** and **61**



$\theta$ (°)	Compound <b>51</b>						Compound <b>61</b>					
	$\Delta E$ ( $\theta_1$ )	$\mu$ ( $\theta_1$ )	$\Delta E$ ( $\theta_2$ )	$\mu$ ( $\theta_2$ )	$\Delta E$ ( $\theta_3$ )	$\mu$ ( $\theta_3$ )	$\Delta E$ ( $\theta_1$ )	$\mu$ ( $\theta_1$ )	$\Delta E$ ( $\theta_2$ )	$\mu$ ( $\theta_2$ )	$\Delta E$ ( $\theta_3$ )	$\mu$ ( $\theta_3$ )
0	13.39	3.97	2.38	2.60	15.62	2.02	0.39	3.26	0.50	3.25	17.34	3.32
15	13.57	4.00	3.01	2.49	15.57	2.00	0.21	3.27	3.29	3.40	10.73	3.52
30	7.20	4.01	3.06	2.55	15.65	1.88	0.31	3.29	4.23	3.52	3.06	3.47
45	2.02	4.01	5.10	2.58	16.46	1.72	1.64	3.31	3.57	3.59	1.66	3.46
60	0.54	3.97	6.75	2.40	18.09	1.54	5.53	3.34	4.85	3.69	2.54	3.44
75	0.89	3.86	6.04	2.34	19.91	1.42	7.03	3.33	4.56	3.80	5.54	3.45
90	1.20	3.63	6.03	2.30	21.81	1.36	5.72	3.28	5.14	3.83	5.07	3.47
105	1.39	3.35	7.43	2.30	20.96	1.43	5.38	3.23	4.58	3.90	3.29	3.49
120	1.51	3.01	9.89	2.35	19.49	1.55	4.13	3.14	5.20	4.03	0.00	3.47
135	1.83	2.66	11.40	2.45	17.78	1.72	2.46	3.04	4.44	4.16	3.34	3.46
150	4.60	2.36	12.23	2.54	18.23	1.94	1.06	2.94	4.86	4.21	11.72	3.42
165	10.36	2.04	15.87	2.58	15.40	2.12	0.28	2.85	10.23	4.09	17.42	3.36
180	9.70	1.71	23.52	2.52	15.47	2.23	0.05	2.80	19.07	3.94	17.61	3.28
195	7.38	1.74	24.69	2.27	14.81	2.23	0.25	2.79	23.65	3.73	18.63	3.15
210	6.33	1.89	25.39	1.98	11.84	2.22	0.96	2.83	15.75	3.58	20.01	3.00
225	2.73	2.44	23.63	1.75	2.90	2.20	2.28	2.90	9.77	3.43	21.21	2.84
240	0.00	2.69	22.05	1.60	0.00	2.14	3.91	2.99	7.01	3.28	21.97	2.74
255	0.13	3.00	14.24	1.46	3.59	2.07	5.15	3.09	6.49	3.13	22.31	2.67
270	0.59	3.34	9.85	1.41	7.40	2.02	5.51	3.17	5.95	3.01	21.28	2.68
285	0.60	3.61	7.10	1.47	10.67	2.00	4.88	3.23	4.68	2.95	21.26	2.72
300	0.26	3.81	4.11	1.62	13.35	1.98	5.37	3.29	3.16	2.94	19.43	2.80
315	0.09	3.94	1.38	1.84	13.63	1.98	1.49	3.29	1.49	2.97	17.85	2.94
330	1.97	3.97	0.00	2.10	14.42	2.00	0.09	3.28	0.28	3.03	19.06	3.12
345	7.21	3.97	0.95	2.43	15.43	2.00	0.00	3.26	0.00	3.13	19.21	3.25
360	13.36	3.97	2.38	2.60	15.62	2.02	0.39	3.26	0.50	3.25	17.34	3.32

<sup>a</sup> Conformational analysis was performed using the semi-empirical PM-3 method available through SPARTAN '08.<sup>18</sup>

<sup>b</sup> Torsion angles ( $\theta_1$ ,  $\theta_2$ ,  $\theta_3$ ) are defined in the structures for **51** and **61** (above) wherein the numbering system is based on X-ray crystal structures shown in in Figure 1A and B, respectively.

<sup>c</sup>  $\Delta E$  (kJ/mol) is the difference between the energy of a conformer and that of the lowest-energy conformer.

<sup>d</sup> Dipole moment ( $\mu$ ) in units of Debye.

defined either way depending on the position of the viewer relative to the molecule.) In addition, the formation of other low-energy conformers at  $\theta_1 = 60^\circ$ ,  $75^\circ$ ,  $255^\circ$ ,  $270^\circ$ ,  $285^\circ$ , and  $300^\circ$  indicates the shallowness of the energy profile in this region of the molecule. The most unstable conformers were formed at  $\theta_1 = 0^\circ$ ,  $15^\circ$ ,  $165^\circ$ , and  $180^\circ$  with  $\Delta = 13.4$ ,  $13.6$ ,  $10.4$ , and  $9.4$  kJ/mol, respectively, relative to the most stable conformer. The calculated energies of the unstable conformers are explained based on the steric interaction between the *ortho*-F atom and the carbonyl oxygen atom when  $\theta_1 = 0^\circ$ , as well as that between the *ortho*-F atom and the  $\alpha$ -hydrogen atom (attached to C12) when  $\theta_1 = 180^\circ$ . Although the magnitude of  $\theta_1$  ( $240^\circ$ ) for the most stable conformer of **51** is different from that found in its crystal structure ( $-32.6^\circ$  or  $327.4^\circ$ ; Table 2), the latter value corresponds to a low-energy (stable) conformation on the solid line in Figure 5A, which is generally expected for a structure found in the solid state.

The conformational analysis around  $\theta_1$  in **51** also predicts, in a general way, the greater stability of the *anti* conformer, relative to that of the *syn* conformer (shown in Scheme 3A). For example, as seen in Table 3, at  $\theta_1 = 0^\circ$  and  $15^\circ$  (roughly corresponding to the *syn* conformation),  $\Delta E(\theta_1) = 13.39$  and  $13.57$  kJ/mol, respectively; both of the latter values correspond to the highest points in the solid-line plot in Figure 5A. On the other hand, the  $\theta_1$  values of  $240^\circ$  (calcd) and  $324^\circ$  (exptl.), representing *anti* conformers of **51**, correspond to the lowest points on the same plot in Figure 5A. In Section 2.1.3, the greater stability of the *anti* conformer relative

to that of the *syn* conformer was attributed to the steric repulsion between the *ortho*-F and the carbonyl oxygen atoms in the latter. This was confirmed by X-ray crystallography whereby it was found that the F...O distance of  $4.048 \text{ \AA}$  in the *anti* conformer is  $4.048 \text{ \AA}$ , as compared to  $2.772 \text{ \AA}$  in the *syn* conformer (calculated for  $\theta_1 = 0^\circ$ ).

Next, we will consider the conformational analysis around the torsion angle  $\theta_2$  in **51**, which is generated by rotation around the C12–C13 bond and is defined by C11–C12–C13–O1 (comprising the enone portion of this molecule). As seen in Figure 5A (dashed line with squares), the most stable conformer is formed at  $\theta_2 = 330^\circ$ , with the next low-energy conformer formed at  $\theta_2 = 345^\circ$  (less stable by  $0.95$  kJ/mol). Overall, the energy profile around  $\theta_2$  is not as shallow as that around  $\theta_1$ . In addition, as compared to  $\theta_1$ , the magnitude of  $\theta_2 = 330^\circ$  (or  $-30^\circ$ ) for the most stable conformer of **51** is in better agreement with that found in its crystal structure ( $-21.7^\circ$  or  $338.3^\circ$ ; Table 2). Furthermore, the conformational analysis around  $\theta_2$  in **51** confirms the general finding that the *s-cis* conformer is more stable relative to the *s-trans* conformer, as shown for chalcone **1** in Scheme 2B. As seen in Table 3 for **51**, at  $\theta_2 = 0^\circ$  (*s-cis* conformer) and  $180^\circ$  (*s-trans* conformer),  $\Delta E(\theta_2) = 2.38$  and  $23.52$  kJ/mol, respectively. The higher value of  $\Delta E(\theta_2)$  for the *s-trans* conformer can be attributed to a repulsive electrostatic interaction between the *ortho*-F and b-H atoms due to a close F...H distance of  $2.320 \text{ \AA}$  as compared to  $4.823 \text{ \AA}$  for the *s-cis* conformer (both calculated by molecular modeling). This

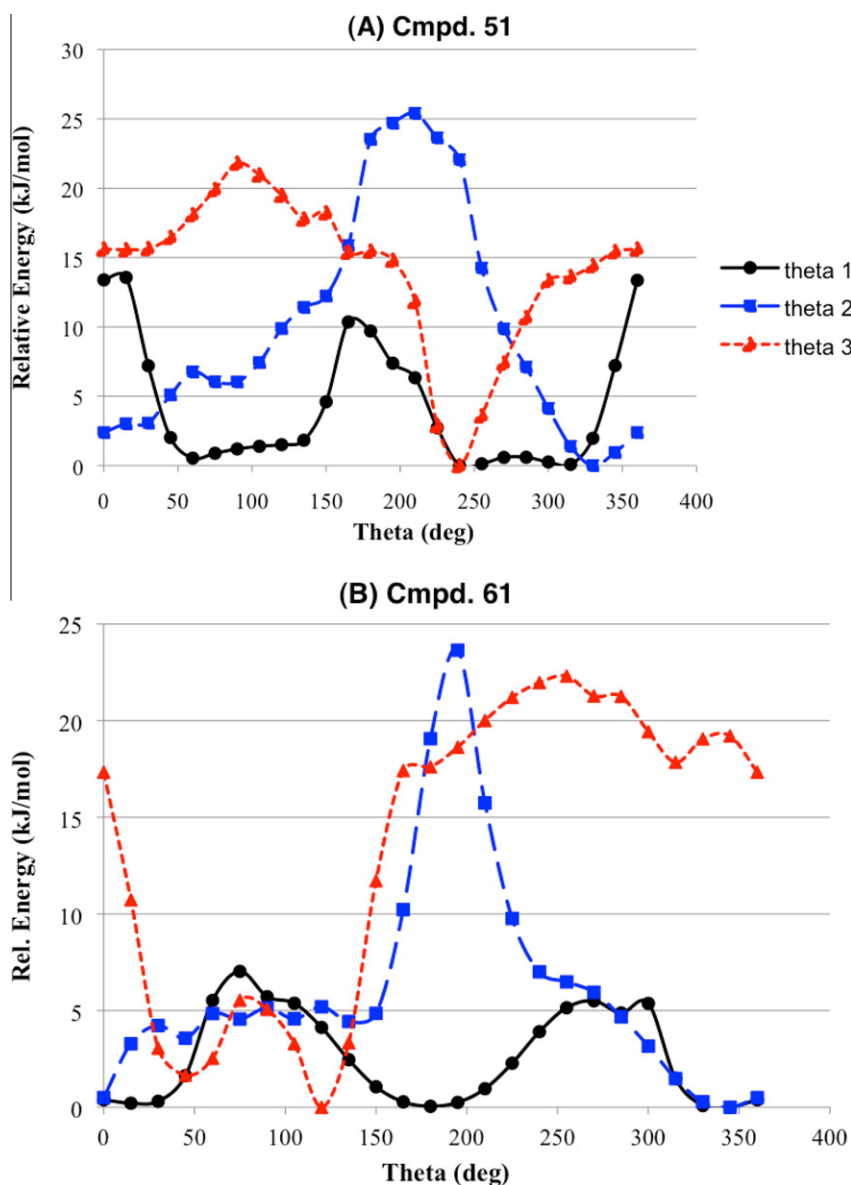


**Figure 5.** Conformational energy profiles as plots of relative energy (kJ/mol) versus torsion angles  $\theta_1$ ,  $\theta_2$ , or  $\theta_3$  for compounds **51** (plot A) and **61** (plot B).

distance is found to be 4.490 Å in the actual solid-state structure of **51**, which is very close to that found for the *s-cis* conformer, thus verifying in a direct manner the validity of the molecular modeling calculations presented here.

Moving on to the torsion angle  $\theta_3$  in **51**, generated by rotation around C6–C11 and defined by C10–C6–C11–C12, we find that the most stable conformer occurs at  $\theta_3 = 240^\circ$ , which differs significantly from that obtained from crystallography ( $-4.4^\circ$  or  $355.6^\circ$ ; Table 2). Similar to the conformational analysis of  $\theta_2$ , the energy profile around  $\theta_3$  is not shallow. Overall, based on the three relative energy curves in Figure 5A, one can conclude that the energy profile of compound **51** is affected the most by the variations in either  $\theta_2$  or  $\theta_3$  as compared to those in  $\theta_1$ .

### 2.3.2. Conformational analysis of compound **61**

We will now consider the energy profile for compound **61**. As shown in Table 3 and Figure 5B (solid line with circles), rotation around the C13–C14 bond (torsion angle  $\theta_1$ , defined by C12–C13–C14–C15) generates many low-energy conformers including the three minima at  $\theta_1 = 345^\circ$ ,  $180^\circ$ , and  $330^\circ$ . As was found for

**51**, the calculated  $\theta_1$  value of  $345^\circ$  in **61** ( $-15^\circ$ ) is very close to that found in its crystal structure ( $-16.3^\circ$ ; Table 2).

Unlike the case of compound **51**, the preference of the *syn* conformation in **61** (i.e., the co-planarity of carbonyl oxygen and furanyl ring oxygen atoms; Scheme 3B) is not immediately obvious from the conformational analysis around  $\theta_1$  in this compound. As mentioned in Section 2.1.3, the observance of a comparable *syn* conformation in a thiophenyl derivative of chalcone has been attributed to an attractive electrostatic interaction between the sulfur atom of the thiophene ring and the oxygen atom of the carbonyl group.<sup>15</sup> However, such an argument would not be useful here since the two atoms in the case of **61** are both oxygens (O···O distance = 2.778 Å by X-ray crystallography) and are thus expected to result in a repulsive interaction. The conformational analysis around  $\theta_1$  in **61** (Table 3) shows that  $\Delta E(\theta_1) = 0.39$  kJ/mol at  $\theta_1 = 0^\circ$  (corresponding to the *syn* conformation), whereas  $\Delta E(\theta_1) = 0.05$  kJ/mol for  $\theta_1 = 180^\circ$  (corresponding to the *anti* conformer). Thus, the *anti* conformer is predicted (via molecular modeling) to be more stable than the *syn* conformer by only 0.34 kJ/mol.

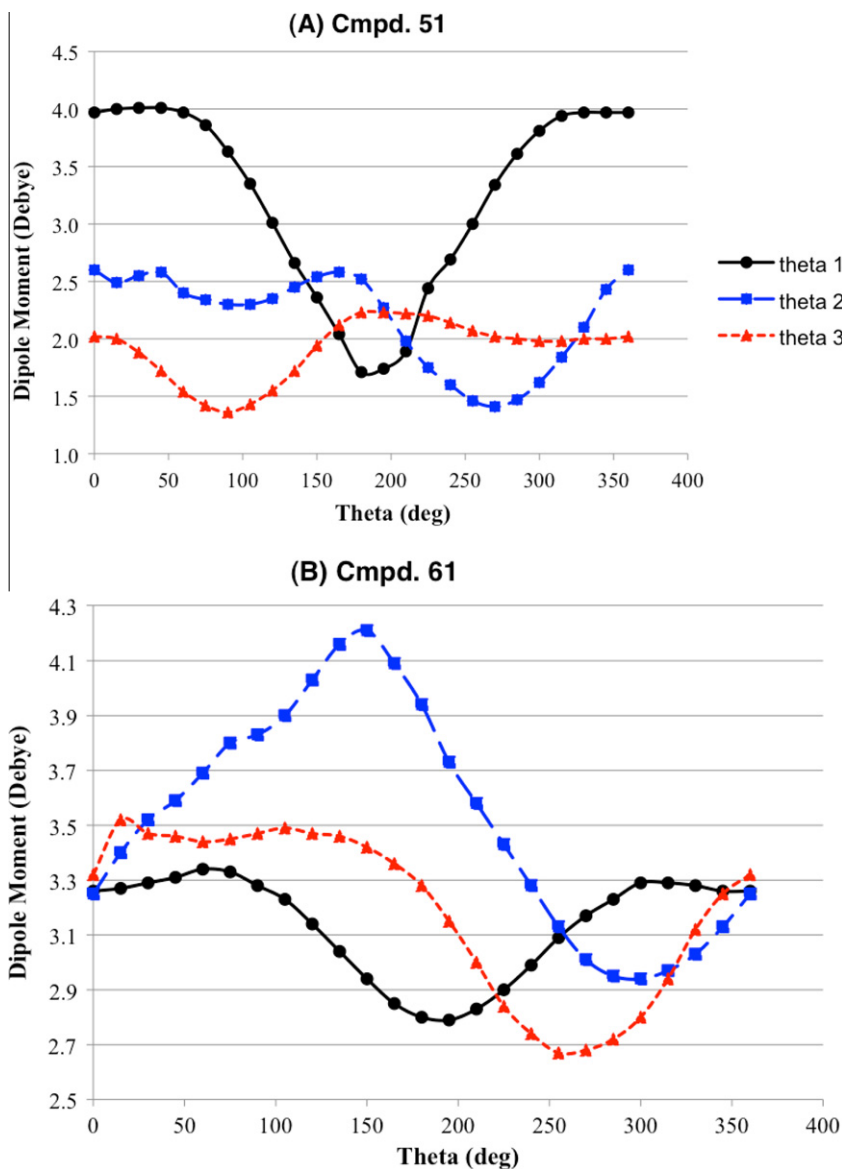
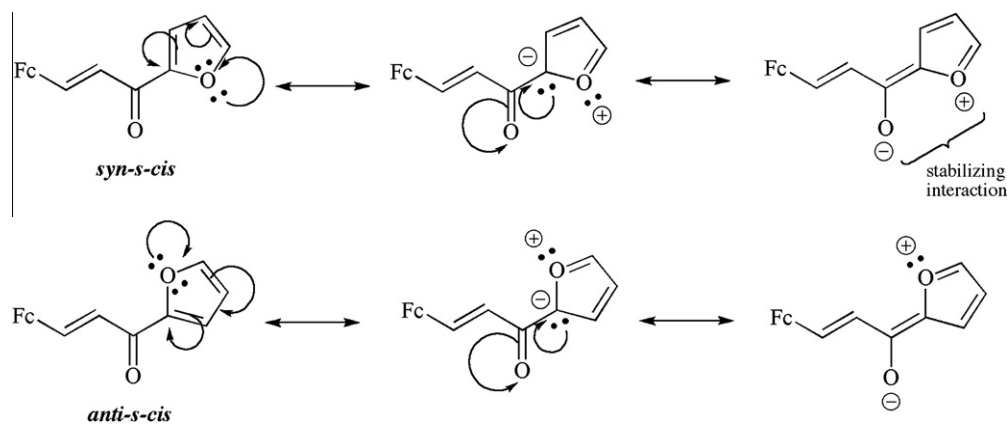


**Figure 6.** Plots of dipole moment versus torsion angles  $\theta_1$ ,  $\theta_2$ , or  $\theta_3$  for compounds **51** (plot A) and **61** (plot B).



**Scheme 4.** Canonical forms of the *syn* and *anti* conformers of **61** showing the favorable electrostatic interaction in the former.

The X-ray crystallographic finding on the preference of the *syn* conformation over *anti*, despite the calculated greater stability (albeit small) of the latter conformer, may be justified by a simple

explanation. As depicted in **Scheme 4**, three canonical forms (among many) may be drawn for each of the two conformers of **61** under discussion. Subsequently, one may argue that the *syn*

conformation in **61** allows for a favorable (stabilizing) electrostatic attraction between the furanyl ring oxygen and the carbonyl oxygen atoms whereas this is not possible for the *anti* conformation. Such interactions have a small effect on the overall stability of the resonance hybrid for each conformer, hence their ready inter-conversion via low-energy rotational barriers.

Rotation around the C12–C13 bond in **61** generates the torsion angle  $\theta_2$  (defined by C11–C12–C13–O1). A plot of  $\Delta E$  versus  $\theta_2$  (Fig. 5B, dashed line with squares) shows two minima at  $\theta_3 = 345^\circ$  and  $0^\circ$ , which are separated in energy by 0.5 kJ/mol. The latter minimum occurs at a  $\theta_1$  value that is very close to that found in the crystal structure of **61** ( $-0.60^\circ$ ; Table 2). Furthermore, as was the case for **51**, the conformational analysis around  $\theta_2$  in **61** confirms again the greater stability of the *s-cis* conformer relative to that of the *s-trans* conformer. As seen in Table 3 for **61**, at  $\theta_2 = 0$  (*s-cis* conformer) and  $180^\circ$  (*s-trans* conformer),  $\Delta E(\theta_2) = 0.50$  and  $19.07$  kJ/mol, respectively. The higher value of  $\Delta E(\theta_2)$  for the *s-trans* conformer can be attributed to a repulsive electrostatic interaction between the *ortho*-H (on the furanyl ring) and b-H atoms at a H...H distance of  $2.090 \text{ \AA}$ , as compared to  $5.115 \text{ \AA}$  for the *s-cis* conformer (both calculated by molecular modeling). This distance is found to be  $5.122 \text{ \AA}$  in the actual solid-state structure of **61**, which is very close to that found for the *s-cis* conformer.

Finally, rotation around the C1–C11 bond in **61** generates the torsion angle  $\theta_3$  (defined by C2–C1–C11–C12). As shown in Figure 5B (dashed line with triangles), there is only one minimum at  $\theta_3 = 120^\circ$ . As was observed for **51**, the conformational profile around  $\theta_3$  in **61** is not shallow (the lowest  $\Delta E$  is at  $2.54$  kJ/mol). In addition, it is observed that among the three torsion angles in **61**,  $\theta_3$  shows the largest discrepancy between the calculated value of the lowest-energy conformer (at  $120^\circ$ ) and that found in the crystal structure ( $-11.2^\circ$  or  $348.8^\circ$ ). As was observed for **51**, it is noted that the conformational energy profile of **61** is also affected the most by the variations in either  $\theta_2$  or  $\theta_3$  as compared to those in  $\theta_1$ .

### 2.3.3. Conformational dipole moment

Another factor that one may consider in a conformational analysis study is the change in the conformational dipole moment ( $\mu$ ) as a function of the three torsion angles mentioned. Dipole moment is an important physical attribute of a molecule since it is directly related to its polarity, a property that can affect both the passage of a molecule through the membrane of a target cell as well as its interaction with a specific enzyme. There have been reports of both experimental<sup>19a,b</sup> and theoretical<sup>19c</sup> work regarding a direct relationship between biological activity of a molecule and its dipole moment. The data obtained on the variation of the conformational dipole moments of compounds **51** and **61** as a function of the three torsion angles are presented numerically in Table 3 and pictorially in Figure 6A and B. The change in the conformational dipole moments of compounds **51** and **61** as a function of the three torsion angles will be discussed below and the possible effect of the molecular polarity of chalcones upon their nematocidal activity will be discussed in Section 2.4.

Each Figure 6A and B is a composite of three plots of dipole moment ( $\mu$ ) versus torsion angles ( $\theta_1$ ,  $\theta_2$ , or  $\theta_3$ ) for compounds **51** and **61**, respectively. For the most part, the six curves in Figure 6A and B have different appearances with some occasional common features. First, although the variation in  $\mu$  as a function of  $\theta_1$  is much more drastic in **51** than that in **61**, varying  $\theta_1$  in both compounds produces similar plots (solid line with circles) wherein the least polar conformer occurs at around  $200^\circ$ . Second, varying either  $\theta_2$  or  $\theta_3$  in **51** and **61** produces very different curves, although the least polar conformer for both compounds occurs at  $\theta_2 \sim 275^\circ$ . Third, the conformational dipole moments for **51** ( $1.41$ – $4.01$  D) encompass a wider range as compared to those for **61** ( $2.67$ – $4.21$  D).

Finally, a comparison of Figures 5A and 6A on the one hand, and of Figures 5B and 6B on the other, reveals an interesting trend among the conformers of **51** and **61**, respectively. For example, if one compares the conformational energy changes for the rotation around  $\theta_1$  in **51** (Fig. 5A, solid line with circles) with those in the conformational dipole moments for the rotation around the same torsion angle (Fig. 6A, solid line with circles), one notices that the minimum in dipole moment curve (at  $\theta_1 = 180^\circ$ ) coincides with a maximum on the relative energy curve. Inspections of other curves in Figures 5A and 6A leads one to the general conclusion that, for compound **51**, the more stable conformers are also more polar. However, analyses of the six curves in Figures 5B and 6B reveals an opposite trend for compound **61**, that is, the more stable conformers are the less polar ones. These findings may have implications in the nematocidal activities of these two compounds (discussed further in Section 2.4).

## 2.4. Structure–activity relationships (SARs)

The apparent structural attributes that seem to be responsible for the biological activity of chalcones against *C. elegans* nematodes in this study will be discussed below.

(1) The placement of the carbonyl group has a profound effect on the biological activity of both organic chalcones and their ferrocenyl analogs, at least with respect to *C. elegans* nematodes. This is reflected in the observation that Type 2 compounds are, in general, more active than those of Type 1 (Fig. 3). This means that, the most active compounds are those where the carbonyl group is attached to the substituted phenyl (or heterocyclic) ring in the organic series, and those where the carbonyl group is not attached to the ferrocenyl group in the Fc-series. Our observations on the nematocidal activities of Fc-chalcones are opposite to those reported by Go and co-workers<sup>6a,b</sup> wherein Type 1 Fc-chalcones were found to show greater antimalarial activity. However, our finding that Fc-chalcones of Type 2 with a heterocyclic ring attached the carbonyl group (i.e., **61** and **62**) are the most active coincides with that of Go et al. since the most active antimalarial compound in their study was found to be **60**. Any observed differences between our results and those obtained by Go et al. may simply be due to the fact that our biological studies were on different species which may point to difference mechanisms and modes of action for these apparently comparable Fc-chalcones.

(2) The lipophilicity of the chalcone may play a significant role in its nematocidal activity. In a study on the antileishmanial activity of a series of organic chalcones, Go et al.<sup>21</sup> found that this activity is associated with less lipophilic organic chalcones while antimalarial activity is associated with more lipophilic ones. In a later study on the antimalarial activity of Fc-chalcones,<sup>6b</sup> Go and co-workers determined the lipophilicity of these types of compounds experimentally from capacity factors measured by reversed-phase HPLC ( $\log k_w$ , pH 7.0). Thus, Fc-chalcones were found to be lipophilic with  $\log k_w$  values in the range  $2.7$ – $5.1$ . In addition, Type 1 Fc-chalcones were found to be less lipophilic ( $\log k_w = 3.63 \pm 0.56$ ,  $n = 15$ ) than their Type 2 analogs ( $\log k_w = 3.87 \pm 0.46$ ,  $n = 15$ ). In addition, it was shown that, in general, Type 1 compounds exhibited greater antimalarial activity than their Type 2 analogs unless Ring B was a substituted heterocycle such as 3-pyridinyl (**60**). This apparent contradictory observation may mean that, at least in the Fc-chalcone series, the magnitude of a compound's lipophilicity may not be a significant predictor of its antimalarial activity. A comparison of this SAR with the apparent SAR observed in our work with respect to *C. elegans* suggests that lipophilicity may indeed be a significant factor in the nematocidal activity of these Fc-chalcones since Type 2 compounds showed higher activity than their Type 1 analogs (Fig. 3A), including the three most effective ones (**50**, **61**, and **62**).

(3) The above discussion on the effect of a chalcone's lipophilicity on its biological activity, coupled with the findings on the trends in conformational energy changes and their corresponding dipole moments in compounds **51** and **61** (as discussed in Section 2.3), prompted us to search for a possible connection between the dipole moment (hence polarity) of a chalcone and its nematocidal activity across the 63-compound series prepared for this study. For this purpose, models of all organic chalcones (**1–30**) and the remaining Fc-chalcones (**31–50**, **52–60**, and **62–63**) were built using SPARTAN '08<sup>18</sup> and their calculated dipole moments were obtained. It was found that the organic chalcones prepared for this study are generally less polar (average  $\mu = 2.86$  D) than their ferrocenyl analogs (average  $\mu = 3.34$  D). This finding should be viewed in light of an earlier statement (Section 2.2.2; Fig. 3) that the organic chalcones, as a class, exhibit higher nematocidal activity compared to Fc-chalcones. In addition, it was mentioned above (Section 2.3) that, for compound **61**, more stable conformers correspond to the less polar ones while the opposite trend is found for **51**. Again, this finding should be viewed in light of the observation that **61** showed much higher nematocidal activity compared to **51**.

There are two complementary explanations for the above findings on the apparent relationship between the molecular polarity and the nematocidal activity of the chalcones. First, the Fc-chalcones may have difficulty passing through the non-polar cell membranes due to their higher polarities as compared to those of the organic chalcones. This rationale may also be used to account for the much higher nematocidal activity of the less polar **61** compared to the more polar **51**. Second, the solvent used for dissolving these chalcones in the biological media prepared to feed the nematodes was DMSO. As a polar, aprotic solvent, DMSO would be expected to stabilize the more polar species. Therefore, Fc-chalcones would then be stabilized in solution relative to their organic counterparts, which translates into the lower reactivity of the former.

(4) The observation that chalcones with aromatic heterocyclic rings attached to the carbonyl group showed very high nematocidal activity in both sets of compounds may suggest that  $pK_a$  values, in addition to lipophilicity, may play an important role in their biological activity.

(5) The presence of the enone portion in the chalcone framework may not be essential for its biological activity. This may be inferred from the spectral data (<sup>1</sup>H NMR, IR) obtained for these compounds (Table 1A and B), which remain relatively unchanged regardless of the variation in their biological activity. Biological activity data in support of this observation has been reported in the literature. For example, Christensen and co-workers<sup>22</sup> found that reduction (or alkylation) of the C=C bond in a series of organic chalcones affects their antimalarial activity only slightly as compared to the potencies of the parent chalcones. On the other hand, Go et al.<sup>6b</sup> found that reduction of the C=C bond in some Fc-chalcones had varied effects upon their antiplasmodial activity, wherein three Type 1 compounds showed reduced activity whereas their Type 2 isomers showed improved activity. These observations may suggest that the enone fragment functions mostly as a spacer between the two aromatic rings, which are the main pharmacophores.

(6) The extent of planarity of the Fc-chalcone molecule seems to play a role in its observed nematocidal activity. This is evident from the results of the X-ray crystallographic study of compounds **51** and **61** obtained in our work, in addition to those obtained by Go et al.<sup>6b</sup> for **37**, **43**, and **58**. The derived torsion angle C12–C13–C14–C15, which reflects the planarity of the enone moiety has a magnitude of  $-32.6^\circ$  and  $-16.3^\circ$  for **51** and **61**, respectively (Fig. 1 and Table 2). The smaller deviation of **61** from planarity can be associated with its higher nematocidal activity (50.8% mortality on day 3) as compared to that of **51** (23.2% mortality on day

3). A similar correlation between planarity of an Fc-chalcone and its biological activity was reported by Go and co-workers<sup>6b</sup> where they found that, for compounds **37**, **58**, and **43**, the magnitudes of the derived torsion angle C12–C11–C1–C2 (reflecting the planarity of the enone moiety) increase in the order  $-3.4^\circ < 163.0^\circ < 170.6^\circ$ , while their antimalarial IC<sub>50</sub> values increase in the order 5.1 mM < 80 mM < 175 mM, respectively. Thus, the most planar Fc-chalcone (among the three studied crystallographically) is also the most active. Therefore, one conclusion that might be drawn here is that, although it might appear that the enone moiety may not play a major direct role in the observed nematocidal activity of Fc-chalcones (as stated in #3 above), one might say that this fragment plays an indirect role in such activity by keeping the whole molecule planar.

(7) The observation that the placement of the ferrocenyl group makes a difference in its biological activity (e.g., Type 1 vs Type 2 for both nematocidal activity and antimalarial activity<sup>6a,b</sup>) leads one to the conclusion that the Fc group does not merely play a bioisosteric role here.<sup>1,2</sup> However, the exact role that this moiety plays in the overall biological activity of Fc-chalcones is poorly understood. Although the incorporation of a ferrocenyl moiety into some molecules with established biological activity (e.g., ferrocifen<sup>3a</sup> and ferrochloroquine<sup>3c–e</sup>) has yielded fruitful results, such incorporation of the Fc group into other well-known classes of compounds such as chalcones has been less successful in terms of increasing the biological activity of the Fc-substituted analogs. It may be, as Go et al.<sup>6b</sup> have also pointed out, that it is an interplay of factors other than the redox properties of the ferrocenyl group (i.e., lipophilicity,  $pK_a$ , and other physicochemical properties) that determines the biological activity of an Fc-chalcone.

## 2.5. Possible mode of action of Fc-chalcones

Although the underlying mechanism for the biological activity of the current set of Fc-chalcones against *C. elegans* is not known, some may be postulated. As suggested by González and Estévez-Braun,<sup>9b</sup> the nematocidal activity of organic chalcones, in general, may result from their role as uncouplers of the oxidative phosphorylation processes in the mitochondria. It seems probable that the ferrocenyl analogs could also act at the mitochondrial level inhibiting or uncoupling respiration.

The mode of action of the Fc-chalcones in nematodes could also result from the electrochemical properties of the Fe<sup>2+</sup> center in the ferrocenyl moiety. In their work with ferrocifen, Jaouen et al.<sup>3a</sup> have proposed that the iron atom, due to its ability to undergo reversible oxidation and reduction, can lead to the formation of ferrocifen-localized hydroxyl radicals as Fe<sup>2+</sup> is oxidized to Fe<sup>3+</sup> by molecular oxygen present in the body. This enables ferrocifen to bind to estrogen receptor proteins, resulting in the subsequent dimerization of these proteins. The attachment of such protein dimers to DNA can halt or reduce the growth of a tumor.

In regards to the DNA binding of Fc-chalcones, Qureshi and co-workers<sup>20</sup> have recently reported on their investigation of such interaction between 1-ferrocenyl-3-(4-nitrophenyl)-2-propen-1-one (**37**, Chart 2) and DNA extracted from chicken blood. Using a combination of experimental techniques such as cyclic voltammetry, UV–vis spectroscopy, and viscometry these authors have determined the binding constant, binding site size, diffusion coefficients, and radii of both free and DNA-bound Fc-chalcone. The results of that study have revealed that (a) the binding interaction is spontaneous, and (b) the intercalation of Fc into DNA is the dominant mode of this interaction. Thus, by analogy, it is quite possible that the nematocidal activity observed for the Fc-chalcones prepared in our work results from the binding of these molecules to the *C. elegans* DNA, which could also explain reproductive inhibition in the nematodes.

**Table 4**  
Crystal data and structure refinement for Fc-chalcones **51** and **61**

	Compound <b>51</b>	Compound <b>61</b>
Empirical formula	C <sub>19</sub> H <sub>14</sub> F <sub>2</sub> FeO	C <sub>17</sub> H <sub>14</sub> FeO <sub>2</sub>
Formula weight	352.15	306.13
Temperature (K)	208(2)	208(2)
Wavelength (Å)	0.71073	0.71073
Crystal system	Orthorhombic	Monoclinic
Space group	<i>Pbca</i>	<i>P2(1)</i>
Unit cell dimensions	<i>a</i> = 7.3656(13) Å, $\alpha$ = 90° <i>b</i> = 11.439(2) Å, $\beta$ = 90° <i>c</i> = 35.139(6) Å, $\gamma$ = 90°	<i>a</i> = 5.828(7) Å, $\alpha$ = 90° <i>b</i> = 11.025(12) Å, $\beta$ = 102.699(15)° <i>c</i> = 10.750(12) Å, $\gamma$ = 90°
Volume (Å <sup>3</sup> )	2960.6(9)	673.8(13)
<i>Z</i>	8	2
Density (calcd) (Mg/m <sup>3</sup> )	1.580	1.509
Absorption coefficient (mm <sup>-1</sup> )	1.041	1.116
<i>F</i> (0 0 0)	1440	316
Crystal size (mm <sup>3</sup> )	0.40 × 0.40 × 0.20	0.15 × 0.07 × 0.05
$\theta$ range for data collection	2.32–28.52°	1.94–27.56°
Index ranges	−9 ≤ <i>h</i> ≤ 4, −15 ≤ <i>k</i> ≤ 14, −44 ≤ <i>l</i> ≤ 46	−5 ≤ <i>h</i> ≤ 7, −14 ≤ <i>k</i> ≤ 9, −13 ≤ <i>l</i> ≤ 11
Reflections collected	18736	3906
Independent reflections	3607 [ <i>R</i> (int) = 0.0566]	2398 [ <i>R</i> (int) = 0.0551]
Completeness to $\theta$ = 25.00°	99.9%	99.3%
Absorption correction	Semi-empirical from equivalents	Semi-empirical from equivalents
Max. and min. transmission	0.8188 and 0.6809	0.9463 and 0.8505
Refinement method	Full-matrix least-squares on <i>F</i> <sup>2</sup>	Full-matrix least-squares on <i>F</i> <sup>2</sup>
Data/restraints/parameters	3607/0/209	2398/1/182
Goodness-of-fit on <i>F</i> <sup>2</sup>	1.092	1.062
Final <i>R</i> indices [ <i>I</i> > 2 $\sigma$ ( <i>I</i> )]	<i>R</i> <sub>1</sub> = 0.0433, <i>wR</i> <sub>2</sub> = 0.1072	<i>R</i> <sub>1</sub> = 0.0787, <i>wR</i> <sub>2</sub> = 0.1992
<i>R</i> indices (all data)	<i>R</i> <sub>1</sub> = 0.0463, <i>wR</i> <sub>2</sub> = 0.1105	<i>R</i> <sub>1</sub> = 0.1033, <i>wR</i> <sub>2</sub> = 0.2138
Extinction coefficient	0.0133(9)	0.009(6)
Largest diff. peak and hole	0.605 and −0.400 (e Å <sup>-3</sup> )	2.235 and −0.735 (e Å <sup>-3</sup> )

### 3. Conclusion

The main goal of this project was to contribute to the database on biological activity of ferrocenyl derivatives of chalcones through a comparative study of a series of such compounds along with their organic analogs. To that end, we have successfully synthesized and characterized a series of 63 compounds, which included 30 organic chalcones and 33 of their ferrocenyl analogs, and have determined their nematocidal activities against the model organism *C. elegans*. Some structure–activity relationships (SARs) have been determined through a combination of spectral (<sup>1</sup>H NMR, IR), X-ray crystallographic, and molecular modeling studies. First, the less polar organic chalcones were found to be much more active against *C. elegans* than their more polar Fc analogs. This indicates that the lipophilicity of a chalcone may play a significant role in its nematocidal activity as it relates to the chalcone's ability to pass through the organism's cell walls. Second, for both the organic and the ferrocenyl series, Type 2 compounds (wherein substituted phenyl group or heterocycle is directly attached to the carbonyl carbon atom) were found to be more active than their Type 1 isomers. Third, the planarity of a chalcone (at least in the Fc series) seems to play a role in its nematocidal activity.

#### 3.1. Future work

There are a few observations that point to possible future directions of this research. (1) One interesting note about this research is that the nematodes treated with the active compounds, for the most part, did not reproduce (i.e., failed to produce embryos). Nematodes that did produce embryos while being treated often died soon after. The nematodes that hatched from these embryos often died soon after as well, suggesting that these particular Fc-chalcones are good nematocides and can inhibit reproduction but are not able to penetrate the protective cuticle on the embryos. Future tests could be run on gravid adult nematodes instead of those in early larval stages to verify that this is the case. (2) One should keep in mind that the model nematode in this study is a free-living species, which

means that these results do not necessarily lead to an effective way of combating plant-pathogenic nematodes. Tests would have to be carried out to determine whether the results obtained for *C. elegans* carry over to other species of nematodes. (3) Concentrations of solution of Fc-chalcones used in our work could not exceed 10<sup>-4</sup> M in order to avoid precipitation of these compounds, thus precluding the possibility of finding a concentration at which all nematodes were killed. Further research is currently underway to determine whether adding hydrophilic substituents to the existing Fc-chalcones can increase their water solubility in an effort to increase the maximum concentration and reduce the amount of DMSO needed. (4) The compounds synthesized for this study do not constitute an exhaustive list of Fc-chalcones by any means. Compounds with other substitution patterns and different heteroatoms could be synthesized and their biological activities investigated in the same way as in this study. Different metals could be used to make different metallocenyl chalcones. Different oxidation/reduction and electronegativity properties of the metals could cause the compounds to have very different biological activities. Also, the ferrocene moiety can be functionalized as well to give very different properties that might be interesting in this study. (5) An important investigation would be to ascertain what environmental impact, if any, would these compounds have. The deleterious effects these compounds have on fish, if any, would need to be established in the event of water contamination. The effects on humans or animals would need to be known in case these compounds happen to be effective against human- or animal-pathogenic nematodes.

### 4. Experimental

#### 4.1. Chemistry

##### 4.1.1. General

All reagents used in syntheses were purchased from commercial sources (Acros or Aldrich) and were used as received without any further purification. <sup>1</sup>H NMR spectra were obtained using a 200-MHz Varian Gemini-2000 spectrometer with CDCl<sub>3</sub> as the solvent.

Chemical shift values ( $\delta$ ) are expressed in ppm and are relative to that of TMS as the internal standard. The multiplicity of each NMR signal is defined as one of the following: s (singlet), d (doublet), t (triplet), q (quartet), dd (doublet of doublets), or m (multiplet). All IR spectra were obtained as thin, dry films on polished NaCl plates (after evaporation of  $\text{CH}_2\text{Cl}_2$  or  $\text{CDCl}_3$  solvent) using a Nicolet Avatar 320 FT-IR spectrophotometer. All melting points were obtained using an Electrothermal Mel-Temp<sup>®</sup> apparatus and are uncorrected. Elemental analyses (C and H only) for the new compounds were performed by Galbraith Laboratories, Inc. (Knoxville, TN).

#### 4.1.2. Synthesis and spectroscopic characterization of chalcones

All syntheses were carried out in the same fashion. Each reaction was monitored by TLC for 24 h to determine when the starting materials had been consumed. All TLC analyses were run on Selecto Scientific flexible silica gel-coated plates containing a fluorescent indicator and were developed using a hexanes–ethyl acetate (4:1) solution as the eluent. The following procedure is representative of the synthesis of all chalcones (see [Charts 1 and 2](#) for structures): A 25-mL round-bottomed flask was charged with the appropriate derivatives of both acetophenone (3 mmol) and benzaldehyde (3 mmol), and mixed with 10 mL of 95% EtOH. The mixture was then stirred magnetically while being gently heated (in a 30 °C water bath) until both starting materials dissolved. In a separate flask, NaOH (3.5 mmol) was added to 10-mL of an ethanol–water (1:1) and the mixture was stirred magnetically until the solid dissolved. The NaOH solution was then added dropwise (using a Pasteur pipet) to the ethanolic solution of acetophenone and benzaldehyde described above. In most cases, the reaction mixture turned yellow and solidified within a few minutes. Ice water (2 mL) was added to the flask and the mixture was stirred vigorously. The solid was collected on a Hirsch funnel, washed with cold water, and air-dried overnight. The purity of the crude product was determined at this point using a combination of TLC analysis, melting point measurement, and <sup>1</sup>H NMR spectroscopy. In case of an oily product, the reaction mixture was extracted with two 10-mL portions of  $\text{CH}_2\text{Cl}_2$  and the organic phase was collected, dried over  $\text{Na}_2\text{SO}_4$ , and removed using a rotary evaporator. The purity of the oily product was then determined as described above. All impure products (solid or oil) were purified by column chromatography using Merck Silica gel (grade 60, 230–400 mesh) and 4:1 hexanes–ethyl acetate as eluent. In case of a solid, chromatographic separation was followed by recrystallization from either methanol or ethanol–water mixture. In all cases, the purity of the final product was checked again as described above; the spectral characteristics were found to be in good general agreement with those found in the literature.<sup>4</sup> The organic chalcones prepared for this study were either pale-yellow solids or oils of the same color (as specified); the ferrocenyl analogs were reddish-orange solids or oils. For each of the reported compounds below, the <sup>1</sup>H NMR data is presented as  $\delta$  (multiplicity, integral ratio), and the IR data as  $\nu_{\text{C=O}}$ ,  $\nu_{\text{C=C}}$ . The following % yield and physical data are for new chalcones prepared for this study. Data for other chalcones (not given below) have been reported elsewhere<sup>4–6</sup> and are also available online as [Supplementary data](#).

**4.1.2.1. (2E)-1-Ferrocenyl-3-(2-methylphenyl)-2-propen-1-one (32).** Yield 90.1%; mp 134–135 °C; <sup>1</sup>H NMR: 7.77 (d, 1H), 7.65–7.57 (m, 2H); 7.42–7.39 (m, 2H), 7.13 (d, 1H), 4.92 (dd, 2H), 4.62 (dd, 2H), 4.21 (s, 5H), 2.40 (s, 3H); IR: 1652, 1595; Anal. Calcd for  $\text{C}_{20}\text{H}_{18}\text{FeO}$ : C, 72.74; H, 5.51. Found: C, 72.79; H, 5.45.

**4.1.2.2. (2E)-1-Ferrocenyl-3-(2-methoxyphenyl)-2-propen-1-one (38).** Yield 89.2%; mp 112–114 °C; <sup>1</sup>H NMR: 8.10 (d, 1H), 7.74–7.66 (m, 2H), 7.38–7.20 (m, 2H), 7.07 (d, 1H), 4.93 (dd, 2H), 4.60 (dd, 2H), 4.23 (s, 5H), 3.90 (s, 3H); IR: 1656, 1581; Anal. Calcd for  $\text{C}_{20}\text{H}_{18}\text{FeO}_2$ : C, 69.38; H, 5.25. Found: C, 69.20; H, 5.31.

**4.1.2.3. (2E)-1-Ferrocenyl-3-(2-diphenylphosphinophenyl)-2-propen-1-one (39).** Yield 69.4%; mp (dec with darkening >100 °C); <sup>1</sup>H NMR: 7.87 (d, 1H), 7.71–6.82 (m, 15H), 4.77 (s, 2H), 4.50 (s, 2H), 4.20 (s, 5H); IR: 1650, 1586; Anal. Calcd for  $\text{C}_{31}\text{H}_{25}\text{FeOP}$ : C, 74.41; H, 5.05. Found: C, 74.17; H, 5.11.

**4.1.2.4. (2E)-1-(2-Methylphenyl)-3-ferrocenyl-2-propen-1-one (44).** Yield 92.3%; mp 134–135 °C; <sup>1</sup>H NMR: 7.50 (d, 1H), 7.27–7.21 (m, 4H), 7.04 (d, 1H), 4.62 (dd, 2H), 4.52 (dd, 2H), 4.19 (s, 5H), 2.40 (s, 3H); IR: 1657, 1589; Anal. Calcd for  $\text{C}_{20}\text{H}_{18}\text{FeO}$ : C, 72.74; H, 5.51. Found: C, 72.63; H, 5.33.

**4.1.2.5. (2E)-1-(2-Chlorophenyl)-3-ferrocenyl-2-propen-1-one (47).** Yield 84.7%; mp 121–123 °C; <sup>1</sup>H NMR: 7.82–7.34 (m, 4H), 7.33 (d, 1H), 6.70 (d, 1H), 4.59 (dd, 2H), 4.51 (dd, 2H), 4.19 (s, 5H); IR: 1639, 1591; Anal. Calcd for  $\text{C}_{19}\text{H}_{15}\text{ClFeO}$ : C, 65.08; H, 4.32. Found: C, 65.29; H, 4.58.

**4.1.2.6. (2E)-1-(3-Chlorophenyl)-3-ferrocenyl-2-propen-1-one (48).** Yield 72.3%; mp 139–141 °C; <sup>1</sup>H NMR: 7.89 (d, 1H), 7.81 (d, 1H), 7.58–7.39 (m, 3H), 7.06 (d, 1H), 4.62 (s, 2H), 4.52 (s, 2H), 4.20 (s, 5H); IR: 1656, 1582; Anal. Calcd for  $\text{C}_{19}\text{H}_{15}\text{ClFeO}$ : C, 65.08; H, 4.32. Found: C, 64.89; H, 4.15.

**4.1.2.7. (2E)-1-(2,4-Dichlorophenyl)-3-ferrocenyl-2-propen-1-one (49).** Yield 97.1%; mp 143–145 °C; <sup>1</sup>H NMR: 7.89 (d, 1H), 7.47 (s, 1H), 7.34 (m, 2H), 7.30 (d, 1H), 6.67 (d, 1H), 4.53 (dd, 2H), 4.50 (s, 2H), 4.17 (s, 5H); IR: 1644, 1584; Anal. Calcd for  $\text{C}_{19}\text{H}_{14}\text{Cl}_2\text{FeO}$ : C, 59.26; H, 3.67. Found: C, 59.02; H, 3.53.

**4.1.2.8. (2E)-1-(2,4-Difluorophenyl)-3-ferrocenyl-2-propen-1-one (51).** Yield 63.4%; mp 105–107 °C; <sup>1</sup>H NMR: 7.94–7.62 (m, 3H), 7.77 (d, 1H), 7.21 (d, 1H), 4.61 (dd, 2H), 4.50 (s, 2H), 4.19 (s, 5H); IR: 1655, 1595; Anal. Calcd for  $\text{C}_{19}\text{H}_{14}\text{F}_2\text{FeO}$ : C, 64.79; H, 4.02. Found: C, 64.63; H, 4.13.

**4.1.2.9. (2E)-1-(2-Methoxyphenyl)-3-ferrocenyl-2-propen-1-one (53).** Yield 80.2%; mp 107–109 °C; <sup>1</sup>H NMR: 7.78 (d, 1H), 7.25–7.19 (m, 4H), 7.08 (d, 1H), 4.64 (s, 2H), 4.52 (s, 2H), 4.19 (s, 5H), 3.90 (s, 3H); IR: 1652, 1595; Anal. Calcd for  $\text{C}_{20}\text{H}_{18}\text{FeO}_2$ : C, 69.38; H, 5.25. Found: C, 69.05; H, 5.13.

**4.1.2.10. (2E)-1-(3,4-Dimethoxyphenyl)-3-ferrocenyl-2-propen-1-one (55).** Yield 66.4%; mp 93–95 °C; <sup>1</sup>H NMR: 7.74 (d, 1H), 7.57 (d, 1H), 7.15 (d, 1H), 6.85–6.93 (dd, 2H), 4.59 (dd, 2H), 4.46 (dd, 2H), 4.17 (s, 5H), 3.98 (s, 3H), 3.95 (s, 3H); IR: 1652, 1575; Anal. Calcd for  $\text{C}_{21}\text{H}_{20}\text{FeO}_3$ : C, 67.03; H, 5.37. Found: C, 67.08; H, 5.23.

**4.1.2.11. (2E)-1-(3,4,5-Trimethoxyphenyl)-3-ferrocenyl-2-propen-1-one (56).** Yield 89.4%; mp 81–83 °C; <sup>1</sup>H NMR: 7.76 (d, 1H), 7.23 (s, 2H), 7.07 (d, 1H), 4.61 (dd, 2H), 4.49 (dd, 2H), 4.19 (s, 5H), 3.96 (s, 3H), 3.94 (s, 6H); IR: 1649, 1570; Anal. Calcd for  $\text{C}_{22}\text{H}_{22}\text{FeO}_4$ : C, 65.03; H, 5.47. Found: C, 64.94; H, 5.62.

**4.1.2.12. (2E)-1-(2-Furanyl)-3-ferrocenyl-2-propen-1-one (61).** Yield 95.1%; mp 107–108 °C; <sup>1</sup>H NMR: 7.79 (d, 1H), 7.60 (s, 1H), 7.24 (s, 1H), 7.02 (d, 1H), 6.53 (s, 1H), 4.56 (dd, 2H), 4.45 (s, 2H), 4.13 (s, 5H); IR: 1644, 1582; Anal. Calcd for  $\text{C}_{17}\text{H}_{14}\text{FeO}_2$ : C, 66.69; H, 4.62. Found: C, 66.85; H, 4.43.

**4.1.2.13. (2E)-1-(2-Thiophenyl)-3-ferrocenyl-2-propen-1-one (62).** Yield 84.9%; mp 116–118 °C; <sup>1</sup>H NMR: 7.80 (d, 1H), 7.52 (s, 1H), 7.18 (s, 1H), 7.03 (d, 1H), 6.49 (s, 1H), 4.61 (s, 2H), 4.50 (s, 2H), 4.19 (s, 5H); IR: 1642, 1575; Anal. Calcd for  $\text{C}_{17}\text{H}_{14}\text{FeOS}$ : C, 63.36; H, 4.39. Found: C, 63.56; H, 4.24.

#### 4.1.3. X-ray crystallography

Suitable crystals of compounds **51** and **61** were obtained by gradual layering of hexanes over a methylene chloride solution of each. Single-crystal X-ray structure determination was carried out at 208(2) K on a Bruker P4 Diffractometer equipped with a Bruker APEX detector. Mo K $\alpha$  radiation ( $\lambda = 0.71073$  Å) was used, and the structure was solved by direct methods with SHELXS-97<sup>23a</sup> and refined by full-matrix least-squares procedures utilizing SHELXL-97.<sup>23b</sup> Crystallographic data collection and refinement information are listed in Table 4. In addition, crystallographic data (excluding structure factors) for structures in this paper have been deposited with the Cambridge Crystallographic Data Center as supplementary publication numbers CCDC 763129 and CCDC 763130 for compounds **51** and **61**, respectively.

#### 4.2. Biology

##### 4.2.1. General

All centrifugations were carried out at 500 rpm and 4 °C using an Eppendorf 5810R centrifuge. Media were prepared as follows: *M-9 buffer solution*: Na<sub>2</sub>HPO<sub>4</sub> (6.44 g, 0.0454 mol), KH<sub>2</sub>PO<sub>4</sub> (1.5 g, 0.0110 mol), NaCl (0.263 g, 0.0045 mol), and NH<sub>4</sub>Cl (0.51 g, 0.0096 mol) were diluted with doubly distilled water to 500 mL. The solution was then autoclaved. *Liquid worm medium*: yeast extract (3 g), peptone (3 g), and dextrose (1 g) were diluted to 100 mL with doubly distilled water. The solution was then autoclaved. Hemoglobin stock (10 mL) and cholesterol (0.8 mL, 5 mg/mL in ethanol) were then added sterilely. *Bleaching solution*: (0.26 M KOH, 1.44% NaOCl in water).

##### 4.2.2. *C. elegans* husbandry

*C. elegans* nematodes were cultured on a plate of nematode growth medium stocked with OP-50 bacteria as a food source. Worms were passed from plate to plate by washing the old plates with M-9 buffer and spotting the resulting suspension onto the fresh plates. The plates were stored in a sterile plastic box in a 25 °C incubator.

##### 4.2.3. Synchronization

The worms were washed in two 5-mL portions into a 15-mL centrifuge tube and centrifuged. The supernatant fluid was removed and 10 mL of a bleaching solution was added. The worms were soaked for 8 minutes with occasional inversion of the tube. The tube was then centrifuged for 5 min at 4 °C. The supernatant fluid was removed and 10 mL of M-9 buffer was added. The tube was centrifuged for 2 min. The supernatant was removed and the M-9 rinse was repeated twice more. The resulting pellet of embryos was then spotted onto a fresh plate stocked with bacteria and allowed to dry.

##### 4.2.4. Preparation of testing solutions and the placement of nematodes

The chalcone to be tested (**1–63**, 10<sup>-4</sup> mol) was placed in a 10-mL volumetric flask and dimethyl sulfoxide (DMSO) was added to the mark. Solution (50  $\mu$ L) was mixed with 4.95 mL of Liquid Worm Medium to give a 10<sup>-4</sup> M solution. Solution (50  $\mu$ L) was pipetted into each well of a 96-well plate and one worm was transferred to each well from the stock plate. Each experiment was performed in triplicate.

##### 4.2.5. Nematode test monitoring

The bioassay was constructed to test the ability of the compounds to kill the worms (% mortality) and inhibit their reproduction (% fecundity). Each test was preformed (in triplicate) in a 96-well plate starting with one nematodes in each well and was observed over a 14-day period (approximate life span *C. elegans*),

during which the percent fecundity (number of nematodes that reproduced) and percent mortality (number of dead nematodes) values were tabulated. Viability of the nematodes was tested under the dissecting microscope by examining each for movement after disturbing it with a probe. Data was collected after 1, 3, 5, 7, 9, 11, 14 days of incubation.

#### 4.3. Molecular modeling

Calculations of conformational energies and dipole moments were performed using the molecular modeling software SPARTAN '08,<sup>18</sup> supported on a MacBook Pro laptop computer. For the detailed conformational analyses of Fc-chalcones **51** and **61** presented in Section 2.3, the starting conformer of each was built within Spartan's interactive building mode with the C=C bond having the *trans* geometry. In addition, the values of the three torsion (dihedral) angles  $\theta_1$ ,  $\theta_2$ , and  $\theta_3$  were constrained to those found by X-ray crystallography for each compound (Table 2). Subsequently, each of the mentioned torsion angles was varied between 0° and 360° (in steps of 15°) while keeping the value of the other two constant (as those of the starting conformer). The strain energy of each conformer so obtained was calculated using the SYBYL force field. The equilibrium geometry of this minimized structure was then recalculated (optimized) using the semi-empirical PM3 method whereby the energy and the dipole moment of each conformer (presented in Table 3) was obtained. The same procedure was followed to calculate the dipole moments of all other chalcones (for the plots in Fig. 6), starting with the *trans* geometry of the C=C bond and the *s-cis* conformation of the enone portion of the molecule.

#### Acknowledgements

(1) The superb technical assistance of Mr. Douglas Kliever with all aspects of spectroscopy is gratefully acknowledged. (2) Two authors (S.A. and A.C.U.) would like to acknowledge the generous support of Dr. Andrew Rogerson, the Dean of the College of Science and Mathematics (CSM) at California State University, Fresno, in terms of funds for release time as well laboratory supplies throughout this project. (3) M.L.G. would like to thank Arnold L. Rheingold of the University of California, San Diego (UCSD), and Charles Campana of Bruker AXS, Inc., for organizing the training workshop, as well as providing useful instruction, through the Crystallography Summer School (July 30–August 8, 2007) during which the X-ray crystallographic data were obtained. She also expresses her gratitude to other course instructors, Richard Staples, Bruce Foxman, Scott Kassel, Kraig Wheeler, and James Golen.

#### Supplementary data

Supplementary data ((a) atomic coordinates (**51**: Table S1; **61**: Table S5); (b) bond lengths and angles (**51**: Table S2; **61**: Table S6); (c) anisotropic displacement parameters (**51**: Table S3; **61**: Table S7); (d) hydrogen coordinates and isotropic displacement parameters (**51**: Table S4; **61**: Table S8); (e) physical characterization of previously reported chalcones (Table S9); (f) packing diagrams for **51** and **61** (Fig. S1); (g) a comparison of mortality and fecundity data for compounds **18** and **50** (Fig. S2); (h) a comparison of mortality and fecundity data for compounds **30** and **62** (Fig. S2)) associated with this article can be found, in the online version, at doi:10.1016/j.bmc.2011.01.048.

#### References and notes

- (a) Jaouen, G. *Bioorganometallics: Biomolecules, Labeling, Medicine*; Wiley-VCH: Weinheim, 2006; (b) Hartinger, C. G.; Dyson, P. J. *Chem. Soc. Rev.* **2009**, *38*, 391.

2. Metzler-Nolte, N.; Salmain, M. In *Ferrocenes Ligands, Materials and Biomolecules*; Stepnicka, P., Ed.; Wiley: West Sussex, 2008; pp 499–639. Chapter 13.
3. (a) Top, S.; Vessières, A.; Cabestaing, C.; Laïos, I.; Leclercq, G.; Provot, C.; Jaouen, G. *J. Organomet. Chem.* **2001**, 637–639, 500; (b) Top, S.; Kaloun, E. B.; Vessières, A.; Laïos, I.; Leclercq, G.; Jaouen, G. *J. Organomet. Chem.* **2002**, 643–644, 350; (c) Biot, C.; Glorian, G.; Maciejewski, L.; Brocard, J. *J. Med. Chem.* **1997**, 40, 3715; (d) Biot, C.; Delhaes, L.; N'Diaye, C. M.; Maciejewski, L. A.; Camus, D.; Dive, D.; Brocard, J. *S. Bioorg. Med. Chem.* **1999**, 7, 2843; (e) Biot, C.; Daher, W.; Ndiaye, C. M.; Melnyk, P.; Pradines, B.; Chavain, N.; Pellet, A.; Fraisse, L.; Pelinski, L.; Jarry, C.; Brocard, J.; Khalife, J.; Forfar-Bares, I.; Dive, D. *J. Med. Chem.* **2006**, 49, 4707.
4. (a) Dahr, D. N. *The Chemistry of Chalcones and Related Compounds*; Wiley: New York, 1981; (b) Liu, M.; Wilairat, P.; Go, M.-L. *J. Med. Chem.* **2001**, 44, 4443; (c) Sivakumar, P. M.; Priya, S.; Doble, M. *Chem. Biol. Drug Des.* **2009**, 73, 403; (d) Quintin, J.; Desrivot, J.; Thoret, S.; Le Menez, P.; Cresteil, T.; Lewin, G. *Bioorg. Med. Chem. Lett.* **2009**, 19, 167; (e) Al Rahim, M.; Nakajima, A.; Misawa, N.; Shindo, K.; Adachi, K.; Shizuri, Y.; Ohizumi, Y.; Yamakuni, T. *Eur. J. Pharmacol.* **2008**, 600, 10; (f) Reddy, M. V. B.; Su, C.-R.; Chiou, W.-F.; Liu, Y.-N.; Chen, R. Y.-H.; Bastow, K. F.; Lee, K.-H.; Wu, T.-S. *Bioorg. Med. Chem.* **2008**, 16, 7358; (g) Gacche, R. N.; Dhole, N. A.; Kamble, S. G.; Bandgar, B. P. *J. Enzyme Inhib. Med. Chem.* **2008**, 23, 28; (h) Alberton, E. H.; Damazio, R. G.; Cazarolli, L. H.; Chiaradia, L. D.; Leal, P. C.; Nunes, R. J.; Yunes, R. A.; Silva, F. R. M. B. *Chem. Biol. Interact.* **2008**, 171, 355; (i) Nozaki, H.; Hayashi, K.-I.; Kido, M.; Kakumoto, K.; Ikeda, S.; Matsuura, N.; Tani, H.; Takaoka, D.; Iinuma, M.; Akao, Y. *Tetrahedron Lett.* **2007**, 48, 8290; (j) Deng, J.; Sanchez, T.; Al-Mawsawi, L. Q.; Dayam, R.; Yunes, R. A.; Garofalo, A.; Bolger, M. B.; Neamati, N. *Bioorg. Med. Chem.* **2007**, 15, 4985; (k) Cabrera, M.; Simoens, M.; Falchi, G.; Lavaggi, M. L.; Piro, O. E.; Castellano, E. E.; Vidal, A.; Azqueta, A.; Monge, A.; Lopez de Cerain, A. *Bioorg. Med. Chem.* **2007**, 15, 3356; (l) Sivakumar, P. M.; Babu, S. K. G.; Mukesh, D. *Chem. Pharm. Bull.* **2007**, 55, 44; (m) Lawrence, N. J.; Patterson, R. P.; Ooi, L.-L.; Cook, D.; Ducki, S. *Bioorg. Med. Chem. Lett.* **2006**, 16, 5844.
5. (a) Biochard, J.; Tirouflet, J. *Compt. Rend.* **1960**, 251, 1394; (b) Frudik, M.; Toma, S. *Chem. Zvesti* **1966**, 20, 326; (c) Perjessy, A. *Chem. Zvesti* **1969**, 23, 343.
6. (a) Wu, X.; Wilairat, P.; Go, M.-L. *Bioorg. Med. Chem. Lett.* **2002**, 12, 2299; (b) Wu, X.; Tiekink, E. R. T.; Kostetski, I.; Kocherginsky, N.; Tan, A. L. C.; Khoo, S. B.; Wilairat, P.; Go, M.-L. *Eur. J. Pharm. Sci.* **2006**, 27, 2175; (c) Zsoldos-Mády, V.; Csámpai, A.; Szabó, R.; Mészáros-Alapi, E.; Pásztor, J.; Hudecz, F.; Sohár, P. *ChemMedChem* **2006**, 1, 1119.
7. (a) Chitwood, D. J. *Annu. Rev. Phytopathol.* **2002**, 40, 221; (b) Bird, D. M.; Kaloshian, I. *Physiol. Mol. Plant Pathol.* **2003**, 62, 115.
8. (a) Thomas, W. *Atmos. Environ.* **1996**, 30, 1; (b) US Environmental Protection Agency Home Page. <http://www.epa.gov/Ozone/mbr> (accessed July 2009); (c) Norman, C. S. *J. Environ. Manage.* **2005**, 75, 167; (d) Norman, C. S.; DeCanio, S. J.; Fan, L. *Global Environ. Chang.* **2008**, 18, 330.
9. (a) Laliberté, R.; Campbell, D.; Brauderlein, F. *Can. J. Pharm. Sci.* **1967**, 2, 37; (b) González, J. A.; Estévez-Braun, A. *Pestic. Biochem. Phys.* **1997**, 58, 193; (c) González, J. A.; Estévez-Braun, A. *J. Agric. Food Chem.* **1998**, 46, 1163.
10. (a) The University of Texas Southwestern Medical Center at Dallas, *Caenorhabditis elegans* WWW Server Home Page. <http://elegans.swmed.edu> (accessed July 2009); (b) Britton, C.; Murray, L. *Int. J. Parasitol.* **2006**, 36, 651.
11. (a) Noack, K.; Jones, N. *Can. J. Chem.* **1961**, 39, 2225; (b) Silver, N. L.; Boykin, D. W., Jr. *J. Org. Chem.* **1970**, 35, 759; (c) Nagy, A. G.; Sohar, P. *J. Organomet. Chem.* **1990**, 390, 217; (d) Venkateshwarlu, G.; Subrahmanyam, B. *Proc. Indian Acad. Sci. (Chem. Sci.)* **1990**, 102, 45; (e) *Interpreting Infrared, Raman, and Nuclear Magnetic Resonance Spectra*; Nyquist, R. A., Ed.; Academic Press: London, 2001. Chapter 14; (f) Thirunarayanan, G.; Gopalakrishnan, M.; Vanangamudi, G. *Spectrochim. Acta, Part A* **2007**, 67, 1106; (g) Yamin, L. J.; Gasull, E. I.; Blanco, S. E.; Ferretti, F. H. *J. Mol. Struct. (Theochem)* **1998**, 428, 167.
12. (a) Go, M. L.; Wu, X.; Liu, X. L. *Curr. Med. Chem.* **2005**, 12, 483; (b) Larsen, M.; Kromann, H.; Kharazmi, A.; Feldbaek Nielsen, S. *Bioorg. Med. Chem. Lett.* **2005**, 15, 4858; (c) Ducki, S.; Forrest, R.; Hadfield, J. A.; Kendall, A.; Lawrence, N. J.; McGown, A. T.; Rennison, D. *Bioorg. Med. Chem. Lett.* **1998**, 8, 1051.
13. *Chemical Abstracts™* and *SciFinder Scholar™* services are available through the Chemical Abstracts Service (CAS, [www.cas.org](http://www.cas.org)), a division of the American Chemical Society. These services are available through a site license at the California State University, Fresno.
14. (a) Son, K.-I.; Noh, D.-Y. *J. Korean Chem. Soc.* **2007**, 51, 591; (b) Jung, Y. J.; Son, K.-I.; Oh, Y. E.; Noh, D.-Y. *Polyhedron* **2008**, 27, 861; (c) Lee, S.-K.; Noh, Y.-S.; Son, K.-I.; Noh, D.-Y. *Inorg. Chem. Commun.* **2010**, 13, 1343.
15. Benassi, R.; Folli, U.; Larossi, D.; Schenetti, L.; Taddei, F.; Musatti, A.; Nardelli, M. *Chem. Soc., Perkin Trans. 2* **1989**, 1741.
16. Hekimi, S.; Lakowski, B.; Barnes, T.; Ewbank, J. *Trends Genet.* **1998**, 14, 14.
17. (a) Xue, Y.; Gong, X. *J. Mol. Struct. (Theochem)* **2009**, 901, 226. and references cited therein; (b) Opletalova, V.; Hartl, J.; Palat, K., Jr.; Patel, A. *J. Pharm. Biomed. Anal.* **2000**, 23, 55.
18. SPARTAN '08 for Mac™; Wavefunction Inc.: Irvine, CA (<http://www.wavefun.com>).
19. (a) Motohashi, N.; Kurihara, T.; Yamanaka, W.; Satoh, K.; Sakagami, H.; Molnar, J. *Anticancer Res.* **1997**, 17, 3431; (b) Kurihara, T.; Motohashi, N.; Sakagami, H.; Molnar, J. *Anticancer Res.* **1999**, 19, 4081; (c) Lopez-Perez, J. L.; del Plmo, E.; de Pascual-Teresa, B.; Merino, M.; Barajas, M.; San Feliciano, A. *J. Mol. Struct. (Theochem)* **2000**, 504, 51.
20. Shah, A.; Qureshi, R.; Khan, A. M.; Ansari, F. L.; Ahmad, S. *Bull. Chem. Soc. Jpn.* **2009**, 82, 453.
21. Go, M.-L.; Liu, M.; Wilairat, P.; Croft, S. L.; Tan, A. L. *Bioorg. Med. Chem.* **2003**, 11, 2729.
22. Nielsen, S. F.; Kharazmi, A.; Christensen, S. B. *Bioorg. Med. Chem.* **1998**, 6, 937.
23. (a) Burla, M. C.; Caliendo, R.; Camalli, M.; Carrozzini, B.; Cascarano, G. L.; De Caro, L.; Gaicovazzo, C.; Polidori, G.; Spagna, R. *J. Appl. Crystallogr.* **2005**, 38, 381; (b) Sheldrick, G. M. *Acta Crystallogr., Sect. A* **2008**, 64, 112.